SFCG Meeting
Rothenburg, Germany
14-23 September 1994

CCSDS - SFCG EFFICIENT MODULATION METHODS STUDY

A COMPARISON OF MODULATION SCHEMES

PHASE 2: SPECTRUM SHAPING

(Response to SFCG Action Item 12/32)

Warren L. Martin
Tien M. Nguyen

Members, CCSDS Subpanel 1E, (RF and Modulation)

August 1994

CCSDS – SFCG EFFICIENT MODULATION METHODS STUDY
PHASE 2: Spectrum Shaping

ACKNOWLEDGMENTS

The authors wish to thank Dr. Sami Hinedi of the Communications Research Section at the Jet Propulsion Laboratory for his invaluable council, suggestions, and discussion of the concepts presented in this paper and for his careful review of the simulation process. Additionally, the authors are in debt to Aseel Anabtawi and Loc Lam for their dedicated effort in preparing the many spectrum plots contained in the following pages and which are the basis for the conclusions reached in this phase of the CCSDS-SFCG Efficient Modulation Methods Study.

The authors convey their special gratitude to Tony Sedor and the other personnel in the Telecommunications and Mission Operations Graphic Arts Department for their heroic efforts in producing all of the drawings, spectra, and other plots contained in this report. Without the dedicated efforts of all of these people this study could not have been completed.

CCSDS – SFCG EFFICIENT MODULATION METHODS STUDY
PHASE 2: Spectrum Shaping

TABLE OF CONTENTS

1.0 INTRODUCTION 1

2.0 OPTIMIZING BANDWIDTH EFFICIENCY 3

2.1 RF Spectrum Management 3
2.1.1 Modulation Schemes 3
2.1.2 Spectrum Shaping 3

2.2 Evaluation of Alternative Systems 4
2.2.1 Simulator Problems 8
2.2.2 Simulation Conditions 8

2.3 Selection of Filter Locations 9

2.4 Optimum Filter Types 12

2.5 Simulation Tests 12

3.0 SIMULATION RESULTS **14**

3.1 Reference Data 14

3.2 Filtered Data 15
3.2.1 Butterworth Filter, 5^{th} Order 15
3.2.2 Bessel Filter, 3^{rd} Order 22
3.2.3 Raised Cosine Filters 22
3.2.3.1 Raised Cosine Filter (α = 0.25), NRZ-L Data 27
3.2.3.2 Raised Cosine Filter (α = 0.5), NRZ-L Data 27
3.2.3.3 Raised Cosine Filter (α = 1), NRZ-L Data 27
3.2.3.4 Square Root Raised Cosine Filter (α = 1), NRZ-L Data 28
3.2.3.5 Raised Cosine Filter (α = 1), Sampled Data 37
3.2.3.6 Square Root Raised Cosine Filter (α = 1), Sampled Data 37

3.3 Summary of Baseband Filter Simulations 38

4.0 SYSTEM CONSIDERATIONS **44**

4.1 Filter Amplitude Response 44
4.1.1 5^{th} Order Butterworth Filter Response 45
4.1.2 3^{rd} Order Bessel Filter Response 46
4.1.3 Raised Cosine Filter Response (α = 1), NRZ-L Data 46
4.1.4 Square Root Raised Cosine Filter Response (α = 1), NRZ-L Data 47
4.1.5 Raised Cosine Filter Response (α = 1), Sampled Data 47

TABLE OF CONTENTS (Continued)

4.1.6 Square Root Raised Cosine Filter Response (α = 1), Sampled Data ... 47
4.1.7 Summary of Filter Output Amplitude Variation Study ... 48

4.2 Inter-Symbol Interference (ISI) ... 50
4.2.1 Raised Cosine and Square Root Raised Cosine Filter Eye Diagrams, NRZ-L Data ... 51
4.2.2 Raised Cosine and Square Root Raised Cosine Filter Eye Diagrams, Sampled Data ... 51
4.2.3 Summary of ISI Studies ... 55

5.0 PHASE 2 SUMMARY ... 56

6.0 PHASE 3 ... 58

REFERENCES ... 59

LIST OF TABLES

1-1 Performance Summaries of Modulation Schemes 2

2-1 Comparison of Theoretical and Simulated Amplitudes 7

2-2 Simulations 13

3-1a Spectrum Levels Relative to First Data Sideband (Ideal Data) 43

31-b Spectrum Levels Relative to First Data Sideband (Non-Ideal Data) 43

4-1 Filter Amplitude Variation to Random Data Pattern 48

4-2 Inter-Symbol Interference for Filter Pairs (Ideal Data and Components) 55

5-1 Summary of Utilization Ratio Improvement 57

LIST OF FIGURES

2-1 Simplified Spacecraft RFS Block Diagram 6

2-2 Frequency Spectra of Random Digital Data (Ideal Data) 7

2-3 Comparison of Traveling Wave Tube and Solid State Amplifiers (Non-Ideal Data) 11

3-1 Spacecraft Configuration for Evaluating Alternative Modulation Methods 16

3-2 Unfiltered Baseband NRZ-L Data Spectra (Ideal Data) 18

3-3 Unfiltered Baseband NRZ-L Data Spectra (Non-Ideal Data) 19

3-4 Baseband 5^{th} Order Butterworth Filtered NRZ-L Data Spectra (Ideal Data) 20

3-5 Baseband 5^{th} Order Butterworth Filtered NRZ-L Data Spectra (Non-Ideal Data) 21

3-6 Baseband 3^{rd} Order Bessel Filtered NRZ-L Data Spectra (Ideal Data) 24

3-7 Baseband 3^{rd} Order Bessel Filtered NRZ-L Data Spectra (Non-Ideal Data) 25

3-8 Amplitude Responses for Raised Cosine Filters 26

LIST OF FIGURES (Continued)

3-9 Baseband Raised Cosine Filtered NRZ-L Data Spectra, (α = 0.25) (Ideal Data) 29

3-10 Baseband Raised Cosine Filtered NRZ-L Data Spectra, (α = 0.25) (Non-Ideal Data) 30

3-11 Baseband Raised Cosine Filtered NRZ-L Data Spectra, (α = 0.5) (Ideal Data) . 31

3-12 Baseband Raised Cosine Filtered NRZ-L Data Spectra, (α= 0.5) (Non-Ideal Data) 32

3-13 Baseband Raised Cosine Filtered NRZ-L Data Spectra, (α = 1) (Ideal Data) 33

3-14 Baseband Raised Cosine Filtered NRZ-L Data Spectra, (α = 1) (Non-Ideal Data) 34

3-15 Baseband Square Root Raised Cosine Filtered NRZ-L Data Spectra, (α = 1) (Ideal Data)..... 35

3-16 Baseband Square Root Raised Cosine (α = 1) Filtered NRZ-L Data Spectra (Non-Ideal Data) 33

3-17 Baseband Raised Cosine Filtered Sampled Data Spectra, (α = 1) (Ideal Data). 39

3-18 Baseband Raised Cosine Filtered Sampled Data Spectra, (α = 1) (Non-Ideal Data) 40

3-19 Baseband Square Root Raised Cosine Filtered Sampled Data Spectra, (α = 1) (Ideal Data)..... 41

3-20 Baseband Square Root Raised Cosine Filtered Sampled Data Spectra, (α = 1) (Non-Ideal Data)..... 42

4-1 Filter Amplitude Responses to a Random NRZ-L and Sampled Data 49

4-2 Eye Diagrams for Raised Cosine Filters (α = 1), NRZ-L Data in a Non-Linear Channel 53

4-3 Eye Diagrams for Raised Cosine Filters (α = 1), Ideal Sampled Data in a Non-Linear Channel 54

CCSDS – SFCG EFFICIENT MODULATION METHODS STUDY
Phase 2: Spectrum Shaping

1.0 INTRODUCTION

At the 12th annual meeting of the Space Frequency Coordination Group (SFCG-12), held during November 1992 in Australia, the SFCG requested the CCSDS RF and Modulation Subpanel to study and compare various modulation schemes (SFCG Action Item 12-32). Preliminary findings were discussed at last year's NASA-ESA Frequency Coordination meeting. The first published report was presented at the CCSDS Subpanel 1E and SFCG meetings in September 1993.

The initial paper considered six modulation schemes including PCM/PSK/PM Square, PCM/PSK/PM Sine, PCM/PM/NRZ, PCM/PM/Bi-ϕ, BPSK/NRZ, and BPSK/Bi-ϕ (Reference 1). It was shown that telemetry subcarriers (PCM/PSK/PM Square or Sine) tend to require an excessive amount of the frequency spectrum. Conversely, PCM/PM/NRZ and BPSK/NRZ are the most spectrum efficient and require the minimum hardware modifications to existing earth station receivers.

While PCM/PM/NRZ and BPSK/NRZ modulation are the most bandwidth efficient, they are sensitive to data imbalance. Therefore, unless convolutional coding is used, care must be exercised to ensure that data balance is maintained [Reference 7]. Modulation systems employing subcarriers were found to be the least efficient and it was concluded that their use should be avoided absent circumstances compelling their use. In fact, based upon that report, the CCSDS has adopted a Blue Recommendation and the SFCG has approved a provisional Recommendation discouraging the use of telemetry subcarriers.

Reference 2 completed Phase 1 of the CCSDS modulation study by reporting the equivalent bandwidth and Inter-Symbol Interference (ISI) results for QPSK, OQPSK, and GMSK modulation. Table 1-1 summarizes the results of the Phase 1 study reported in References 1, 2, and 8.

This paper is concerned with Phase 2 of the *CCSDS -SFCG Efficient Modulation Methods Study* and explores the benefits accruing from spectrum shaping of the transmitted signal. Several alternative filter types and locations are considered and the results are compared. An estimate of the increased spectrum utilization, resulting from the application of the proper modulation and spectrum shaping methods, is provided. It is shown that spectrum shaping, in combination with an efficient modulation type, has the potential for increasing frequency band utilization by several times.

TABLE 1-1: PERFORMANCE SUMMARIES OF MODULATION SCHEMES

Modulation Type	90% Power Containment	95% Power Containment	ISI SNR Reduction dB	ISI SNR Reduction dB	ISI SNR Reduction DB	In-Band Interference Susceptibility
PCM/PSK/PM (Sq)[1] n=9, m=1.2 rad.	± 30 R_B	± 75 R_B	0.75 @ ± 10 R_B	0.15 @ ± 20 R_B	0.01 @ ± 50 R_B	Less susceptible than PCM/PSK/PM sine by about 4 dB. Susceptible to Out-of-Band interference.
PCM/PSK/PM (Sine)[1] n=9, m=1.2 rad.	± 10 R_B	± 10 R_B	0.75 @ ± 10 R_B	0.18 @ ± 20 R_B	0.04 @ ± 50 R_B	More susceptible than PCM/PSK/PM square.
PCM/PM/Bi-ϕ[1] m=1.2 rad.	± 2.9 R_B	± 5.1 R_B	6.3 @ ± 1 R_B	0.34 @ ± 2 R_B	0.20 @ ± 5 R_B	No information available.
PCM/PM/NRZ[1] m=1.2 rad.	± 0.7 R_B	± 1.2 R_B	0.85 @ ± 1 R_B	0.21 @ ± 2 R_B	0.01 @ ± 5 R_B	No information available.
BPSK/Bi-ϕ m=± 90 deg.	± 3.1 R_B	± 6.5 R_B	6.3 @ ± 1 R_B	0.29 @ ± 2 R_B	0.15 @ ± 5 R_B	Less susceptible than QPSK. No information available comparing to modulation types listed above.
BPSK/NRZ m=± 90 deg.	± 1 R_B	± 2 R_B	0.74 @ ± 1 R_B	0.17 @ ± 2 R_B	0.04 @ ± 5 R_B	Likely to be more sensitive than BPSK/Bi-ϕ. No information available as to other modulation types.
QPSK	± 0.5 R_B	± 1.0 R_B	0.35 @ ± 0.5 R_B	0.2 @ ± 1.0 R_B	-	More sensitive than BPSK/NRZ due to crosstalk and phase distinguishability.
OQPSK	± 0.5 R_B	± 1.0 R_B	0.15 @ ± 0.5 R_B	0.1 @ ± 1.0 R_B	-	More sensitive than BPSK/NRZ due to crosstalk and phase distinguishability.
GMSK	± 0.4 R_B	± 0.5 R_B	0.35 @ ± 0.4 R_B	0.2 @ ± 0.5 R_B	-	Similar to MSK [Ref. 8} (i.e., less sensitive than BPSK/NRZ).

NOTES:

1. 13.1% of power contained within residual carrier.
2. R_B is the frequency span occupied by each data bit, given the data bit rate (R_B) is the same as R_S in Phase 1

2.0 OPTIMIZING BANDWIDTH EFFICIENCY

This paper documents the work completed since the SFCG meeting in late September 1993. At the conclusion of these modulation studies, Recommendations will be drafted by the CCSDS and SFCG endorsing specific modulation types and spectrum shaping depending upon mission conditions.

2.1 RF Spectrum Management

From the Phase 1 findings, it became obvious that careful selection of the modulation type, together with some spectrum shaping, will be required to achieve bandwidth efficient communications.

2.1.1 Modulation Schemes

Phase 1 concluded that spectrum utilization is very dependent upon modulation type (References 1 and 2). With these studies, nine modulation schemes were investigated and their characteristics are summarized in Table 1-1. It was shown that telemetry subcarriers (PCM/PSK/PM Square or Sine) tend to require an excessive amount of the frequency spectrum. Conversely, GMSK, OQPSK, QPSK, BPSK/NRZ, and PCM/PM/NRZ are the most spectrum efficient. GMSK is clearly the most bandwidth efficient modulation method although the remaining four modulation types listed above produce acceptable Inter-Symbol-Interference (ISI) levels when band limited to $\pm$ 2 x Data Rate (R_B). (R_B is the frequency span occupied by one bit given the data rate and is equivalent to R_S in the Phase 1 paper.)

2.1.2 Spectrum Shaping

Judicious filtering can also assist in reducing spectrum utilization. When used in conjunction with a spectrum efficient modulation, the result can be a significant savings in the *Required Bandwidth*. The issue becomes one of selecting the proper filter type and location.

Spectrum shaping increases the risk of Inter-Symbol Interference (ISI). Band-limiting caused by the filter distorts the symbol's waveform so that successive symbols begin to overlap one another resulting in ISI [Reference 9]. It is not sufficient to shape the spacecraft's transmitted spectrum such that it requires only a small portion of the RF frequency band if the result significantly increases the ISI. ISI appears as a telemetry data system loss and should be accounted for under *Waveform Loss* on page 4 of the CCSDS Link Design Control Table (DCT).

Accordingly, any spectrum shaping investigation must consider the additional losses due to ISI for it is a major parameter establishing the utility of each modulation scheme. Furthermore, nonlinearities found in the spacecraft's modulator, multiplier and power amplifier, along with imperfect data, can introduce

additional spurious emissions, including in-band components, into the transmission. These factors must also be considered in order to obtain a reasonable evaluation of the overall system. This study's objective is to provide the most realistic estimate of actual system performance possible without building and testing real hardware.

Figure 2-1 is a simplified block diagram of a Spacecraft Radio Frequency Subsystem (RFS). It identifies three locations where spectrum shaping can occur (shaded boxes) which will limit the *Required Bandwidth* of the transmitted signal. These are: 1) At the input to the spacecraft's modulator, 2) At the output of the multiplier, and 3) At the output of the power amplifier. Baseband filtering is always used in the turnaround transponder's ranging channel so there will be no further consideration of its characteristics. The following Sections discuss the merits of placing the filters at these three locations.

2.2 Evaluation of Alternative Systems

Evaluating alternative implementation approaches, using only analytical methods, is probably an exercise in futility. Unless one assumes virtually perfect conditions (e.g., data and hardware), the number of factors to be considered becomes unmanageable. Ideally, one would build the required hardware and make actual measurements on each of the several systems. However, this approach is clearly impractical from both a cost and time approach.

Thus, it was decided to utilize a communications system simulator. While not a perfect emulator of a real system, it does provide a close approximation permitting the comparative studies to be completed in a finite amount of time. Its accuracy should be far greater than a purely analytical approach, particularly if care is exercised in modeling the several system elements.

The system utilized was a Signal Processing Worksystem (SPW) marketed by COMDISCO Systems, Foster City, California. This software is installed on a SPARC-10 Sun Workstation. COMDISCO has a library of communications system components. For this study, JPL spacecraft modulator and frequency multiplier models were employed. These two models are based upon specifications and information describing the same components found in the NASA Standard Transponder.

Simulations were completed using ideal and non-ideal data. Ideal data exhibits perfect symmetry and data balance while non-ideal data conforms to the CCSDS Recommendations 401 (2.4.8) B-l for asymmetry and to Recommendation 401.0 (X.X.X) B-l for data imbalance. The CCSDS limits data asymmetry (ratio of time duration of a 1 to time duration of a 0) to $\pm$ 2% and data imbalance (probability of a 1 vs. probability of a 0 [mark-to-space ratio]) to 0.45. **Except for the Raised Cosine and Square Root Raised Cosine filters (α = 1), which received both NRZ-L and Sample data inputs, all simulations used NRZ-L inputs since most spacecraft data systems produce that format.**

Non-ideal data was used so that the simulation results would more accurately predict actual hardware performance. Stray capacitance in spacecraft wiring can increase the data asymmetry while the random data can produce long runs of 1s or 0s (data imbalance). Data imbalance will not pose a problem with PCM/PM/Bi-ϕ modulation, since each data symbol will have both states (1 and 0). However, for PCM/PM/NRZ modulation, data imbalance is a significant concern [Ref. 7].

Initially, concern was expressed regarding the accuracy of the COMDISCO simulator. Users of different software had discovered that their simulations contained errors in the amplitude of the modulation sidelobes, which were several R_B away from the carrier. It was reported that the COMDISCO simulation of ideal data could be 5 dB below the correct level at $f_C \pm 10\ R_B$.

To calibrate the accuracy of the COMDISCO system, a frequency spectrum of ideal, random data was made. Figure 2-2 and Table 2-1 contain the results of both theoretically computed and simulated amplitudes. Note the good agreement indicating that COMDISCO accurately simulates frequency spectra amplitudes.

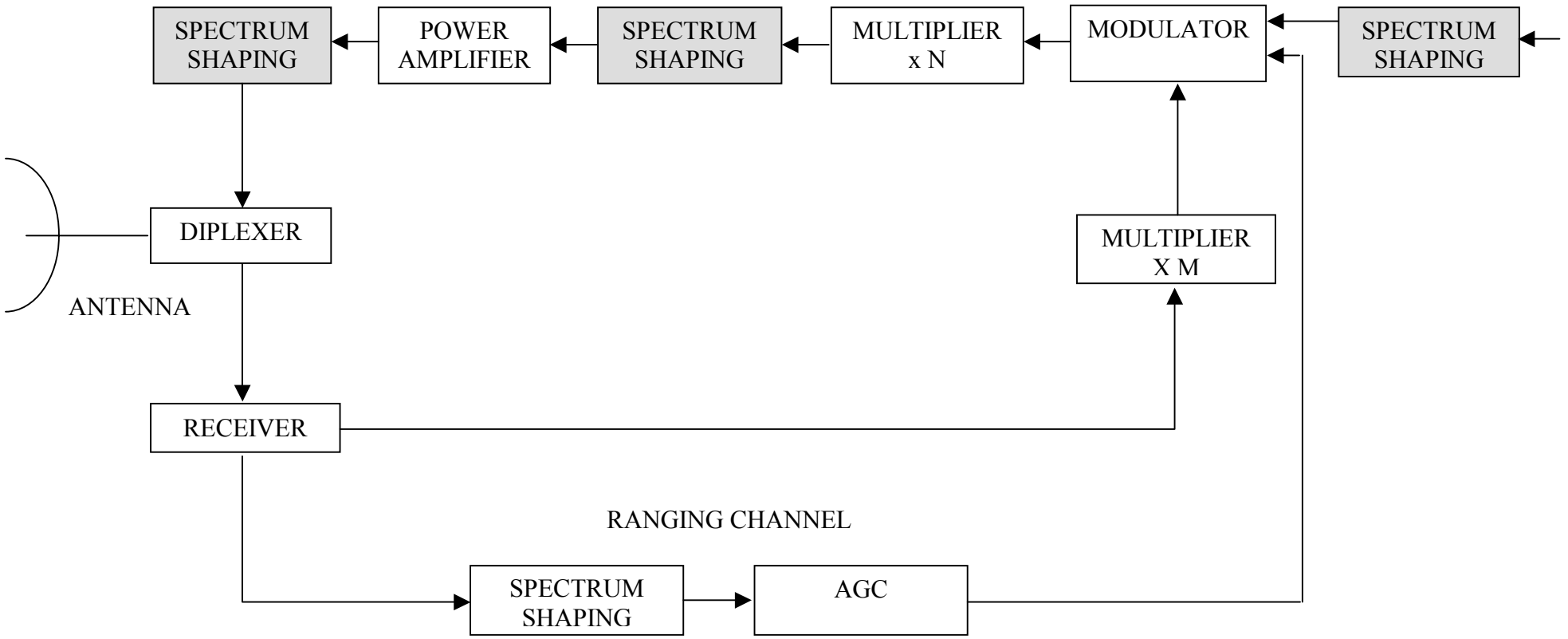

Figure 2-1. Simplified Spacecraft RFS Block Diagram

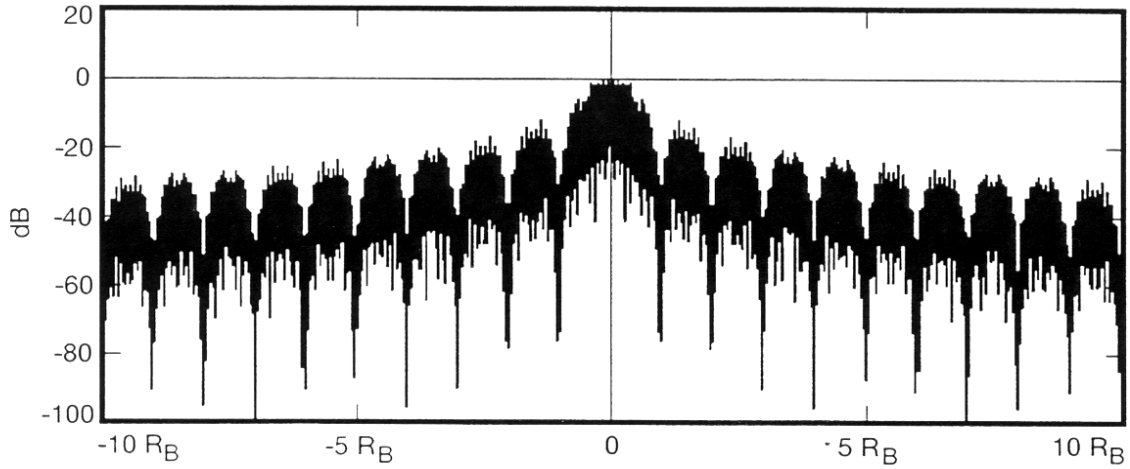

Figure 2-2. Frequency Spectrum of Random Digital Data (Ideal Data)

Table 2-1. Comparison of Theoretical and Simulated Amplitudes

Offset from Center Frequency ($\pm R_B$)	Theoretical Amplitude (dB)	Simulated Amplitude (dB)
0	0	0
1.5	-13.46	-13.5
2.5	-17.90	-18
3.5	-20.82	-21
4.5	-23.01	-23
5.5	-24.75	-25
6.5	-26.20	-27
7.5	-27.44	-27.5
8.5	-28.53	-29
9.5	-29.50	-29.5

Figure 2-2 and Table 2-1. COMDISCO Simulation of Random Data Spectrum

2.2.1 Simulator Problems

COMDISCO's simulation software used in JPL's Communications Research Section (331) contains models for a modulator, a multiplier, a TWT power amplifier, and now, a solid-state power amplifier. All models emulate real equipment and contain the nonlinearities and imperfections found in the actual hardware.

The modulator and multiplier models were designed by JPL and are based upon characteristics of corresponding elements found in NASA's standard deep space transponder. COMDISCO provided the model for the TWT, which replicates a Hughes TWT Mode1275H. JPL implemented the Solid State Power Amplifier (SSPA) model, which is based upon specifications provided by the European Space Agency (ESA) for their 10 Watt, solid-state, S-band power amplifier.

Some problems arose during the simulations due to differing conventions. COMDISCO designed their model of the Hughes 275H TWT to operate with a baseband complex envelope input/output and then be translated to the RF carrier frequency. Their reasoning was simple. Computers function slowly and have limited capacity. By operating at baseband, the sample rate-to-modulation data rate ratio, and hence the resolution, can be greatly increased over that which would be possible at the full RF frequency. All imperfections and nonlinearities found in the actual TWT have been translated to baseband and are included in the model.

Conversely, the modulator and multiplier models were designed to operate at the full RF frequency so that a complete RF simulation could be obtained, although at a lower resolution. When this difference was discovered, models for the modulator, multiplier and new solid state power amplifier were translated to also operate at baseband. Like the TWT, all imperfections inherent in the actual hardware operating at RF frequencies are retained in the revised models.

All simulations utilize both ideal and non-ideal NRZ-L and Sampled data as defined in Section 2.2. Additionally, a non-ideal modulator, multiplier, and 10 Watt solid state S-band amplifier were employed to ensure that the results represent actual system performance. Simulations were made at baseband and translated to the RF operating frequency.

2.2.2 Simulation Conditions

Because of the large number of simulations required, it was decided to focus on a single modulation scheme for Phase 2. Although not the most bandwidth efficient, PCM/PM/NRZ modulation was selected because most space agencies still use residual carrier communications systems. While implemented only occasionally,

the bandwidth efficiency of PCM/PM/NRZ makes it attractive for evaluating filter efficacy.

Efficient spectrum utilization is most important for Category A missions where their larger numbers, stronger signals, and higher data rates exacerbate the frequency band congestion. Therefore, where possible, Phase 2 focused on these systems rather than on those used for Category B missions where congestion is less of a problem. Consequently, all simulations employed the ESA 10 Watt solid state power amplifier and a 4^{th} Order Butterworth bandpass second harmonic filter, with a $\pm$ 20 R_B cutoff frequency, following the power amplifier (Figure 2-1). (R_B is the frequency spectrum width required by a single data bit).

For comparative purposes, spectra for both the Hughes TWT Model 275H and the European Space Agency's 10 Watt Solid State S-band power amplifiers are provided in Figure 2-3 using a spectrum width of $f_C \pm 20\ R_B$. Both amplifiers were operating in full saturation. Spectra for the two amplifier types, using non-ideal data, showed no discernable differences. Accordingly, the following results are believed to be equally applicable to both TWTs and solid state amplifiers, operating in a fully saturated mode.

As noted, models for a non-ideal modulator and multiplier were also utilized. These models are estimates of the modulator and multiplier found in the NASA standard transponder an are based on published specifications. When combined with non-ideal data, the simulation should represent actual spacecraft telemetry system performance reasonably well.

2.3 Selection of Filter Locations

Figure 2-1 shows that filters can be placed at the modulator's input, the multiplier's output, and/or the power amplifier's output. Clearly, from a spectrum management viewpoint, the most effective filter location is following the power amplifier. Such a filter will attenuate spurious emissions resulting from nonlinearities in the modulator, multiplier, and power amplifier. Moreover, all spacecraft should have 2^{nd} harmonic filters to reduce unwanted emissions in other bands.

However, from a spacecraft construction and operations perspective, spectrum shaping following the power amplifier is undesirable. Not only do such filters have to carry the full transmitted power, which tends to make them large and heavy, but also, output filtering may not be compatible with some mission operations requirements.

For example, unless the telemetry symbol rate is equal to, or greater than, the ranging code rate, the filter's bandwidth will be a compromise either partially attenuating the ranging signal and/ or permitting far too many telemetry data sidebands to be transmitted defeating the objective of limiting the telemetry spectrum. Such a filter is likely to preclude Δ DOR measurements.

There is yet a third disadvantage to an output filter. An output filter can significantly reduce the high order data sidebands together with any spurious emissions that may be present. However, a portion of the transmitted power is contained within the data sidebands and their elimination translates into a power loss. In the past, a 5% loss (-0.2 dB) was considered to be acceptable.

Some filtering at the power amplifier's output will be required to eliminate the second, and higher order harmonics generated by the nonlinearities present in the power amplifier. Perhaps in some cases, this filter can also be used to partially filter the data sidebands. However, it should be expected that such sideband filtering will be modest.

Therefore, other filter locations should be considered. Again, from a spectrum management viewpoint, the second most desirable location is following the multiplier and just prior to the power amplifier. This is so because artifacts resulting from nonlinearities in the modulator and multiplier will be reduced even if those from the power amplifier will not. Spectrum shaping at the multiplier or power amplifier input may be necessary in BPSK and/or QPSK systems using "switched modulators" where baseband filtering is not feasible (see page 10 and Section 4.1.3). With suppressed carrier modulation, ranging and Δ DOR tones are unlikely to pose problems and these filter locations should be acceptable. To obtain the same performance measured for the baseband filters, the bandpass characteristics should produce same transmitted RF spectrum characteristics discussed on the following pages.

Baseband filtering remains as the single, most advantageous, alternative to post power amplifier filtering for residual carrier modulation. Virtually all of the disadvantages listed above for the post power amplifier filter are eliminated. The filter can be small, lightweight, and consume very little power. Moreover, such a filter location is compatible with simultaneous telemetry, ranging, and Δ DOR tones since they can have separate, unfiltered, modulator inputs.

However, baseband filtering may be incompatible with some suppressed carrier modulators. Lithe BPSK or QPSK modulator is linear so that its output phase shift is a linear function of input voltage, then baseband filtering is feasible. Conversely, if the modulator is "switched" so that the output phase has 2 (BPSK) or 4 (QPSK) discrete phases which occur when the input voltage passes certain thresholds, or if a digital input is required, then baseband filtering will not be effective.

Baseband filtering suffers from one other significant disadvantage. Irrespective of how well the input data has been filtered, nonlinearities found in the modulator, multiplier and solid state power amplifier will have a tendency to reestablish the data sidebands that the filter was intended to eliminate. Nevertheless, because of its simplicity, an investigation of baseband filtering is worthwhile to quantify the benefits, which can be obtained.

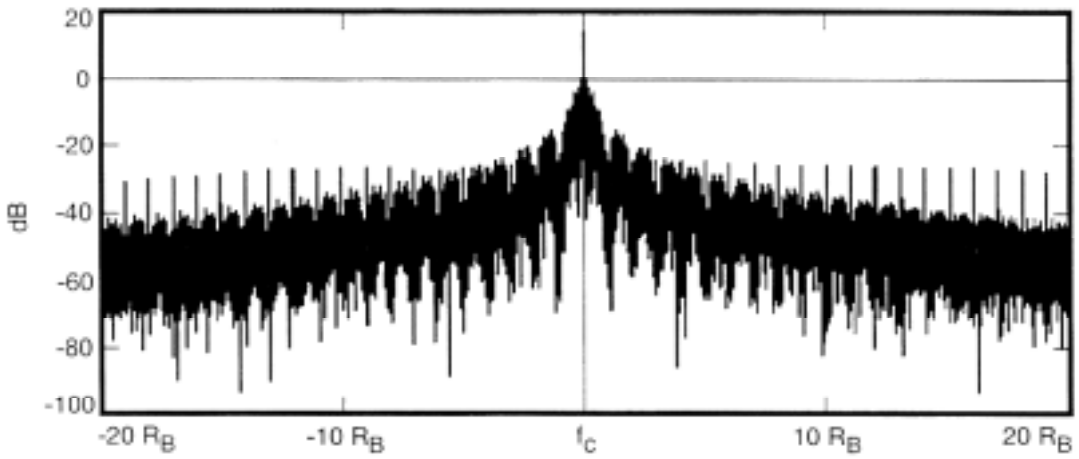

Figure 2-3a. Solid State Power Amplifier (SSPA) Spectrum (Non-Ideal Data)

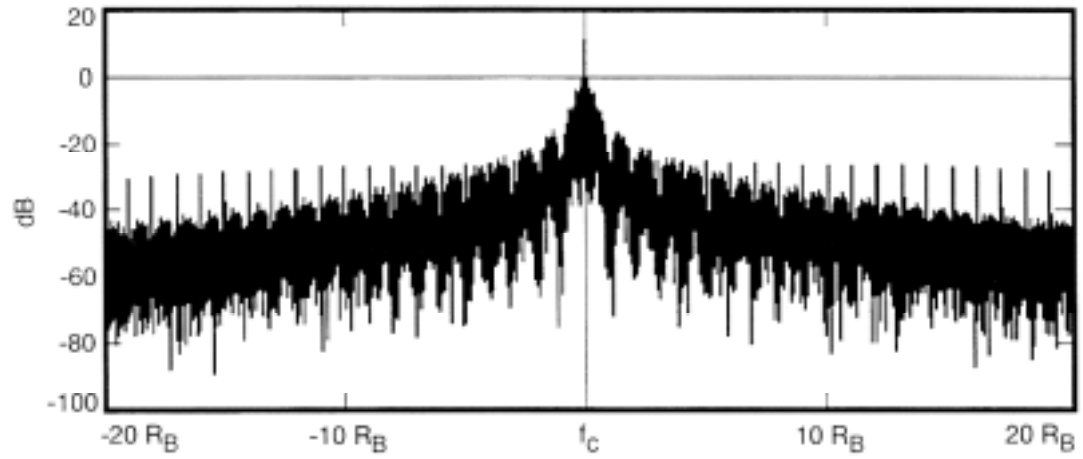

Figure 2-3b. Traveling Wave Tube (TWT) Spectrum (Non-Ideal Data)

Figure 2-3. Comparison of Traveling Wave Tube and Solid State Power Amplifiers (Non-Ideal Data)

2.4 Optimum Filter Types

Given that baseband filtering is the most practical choice, one must select the optimum filter type for this location. This selection is especially critical because of the several nonlinear elements following the filter. As noted above, each of these elements has a tendency to restore some of the frequency components that the filter removed. Moreover, some filters exhibit ringing at the cut-off frequency which wreaks havoc when passed through non-linear system components.

Here, the approach was to simulate the system's performance using the equipment described in Section 2.2.2 which included models of a non-ideal modulator, multiplier, and power amplifier. Four filter types were selected for comparison. These were: a 5^{th} Order Butterworth filter, a 3^{rd} Order Bessel filter, Raised Cosine filters with α = 0.25, 0.5, and 1, and a Square Root Raised Cosine filter with α = 1.

Note: The purpose of these simulations was to establish the effect of baseband filtering on the transmitted data's spectrum. Accordingly, narrow bandpass filters were used with cut-off frequencies of $\pm$ 1 R_B. (1 R_B is the span of a single data bit in the frequency domain, e.g., for random data, spectral nulls occur at $\pm$ 1 R_B, $\pm$ 2 R_B, ….$\pm$ n R_B).

One might expect that the Inter-Symbol Interference (ISI), resulting from such a narrow baseband filter, might be high. In Phase 1 of this study, it was found that filter bandwidths of at least $\pm$ 2 R_S [$\pm$ 2 R_S = $\pm$ 2 R_B] were required to ensure that the ISI was held to an acceptable value.

2.5 Simulation Tests

Table 2-2 contains a list of the simulations undertaken for this study. Because of time constraints, all simulations employed a PCM/PM/NRZ modulation format. The first two simulations, without any baseband filtering, were intended to serve as references with which to compare subsequent simulations employing a variety of baseband filters. Each of the reference spectrum plots should be compared with the corresponding plots for the filtered data in order to evaluate the benefits o baseband filtering. These first two cases utilize ideal data (no data asymmetry nor any data imbalance) and non-ideal data (corresponding to characteristics set forth in Section 2.2 respectively)

CCSDS – SFCG EFFICIENT MODULATION METHODS STUDY
Phase 2: Spectrum Shaping

Table 2-2: SIMULATIONS

Sim. No.	Modulation Type	Filter Location	Filter Type	Filter Char.	Data Char.	Spectrum Plots	Plot Locations	Test Purpose
1	None (Baseband)	None	None	None	Ideal NRZ-L	± 10 R_B, ± 200 R_B	Mod, PA, PA Unfil.	Unfiltered NRZ-L data spectrum reference.
2	None (Baseband)	None	None	None	Non-Ideal NRZ-L	± 10 R_B, ± 200 R_B	Mod, PA, PA Unfil.	Unfiltered NRZ-L data spectrum reference.
3	PCM/PM/NRZ	Baseband	Butterworth	5th Order	Ideal NRZ-L	± 10 R_B, ± 200 R_B	Mod, PA, 2nd Har Fil	Evaluation of Butterworth filter, ideal NRZ-L data.
4	PCM/PM/NRZ	Baseband	Butterworth	5th Order	Non-Ideal NRZ-L	± 10 R_B, ± 200 R_B	Mod, PA, 2nd Har Fil	Evaluation of Butterworth filter, non-ideal NRZ-L data.
5	PCM/PM/NRZ	Baseband	Bessel	3rd Order	Ideal NRZ-L	± 10 R_B, ± 200 R_B	Mod, PA, 2nd Har Fil	Evaluation of Bessel filter, ideal NRZ-L data.
6	PCM/PM/NRZ	Baseband	Bessel	3rd Order	Non-Ideal NRZ-L	± 10 R_B, ± 200 R_B	Mod, PA, 2nd Har Fil	Evaluation of Bessel filter, non-ideal NRZ-L data.
7	PCM/PM/NRZ	Baseband	Raised Cosine	$\alpha = 0.25$	Ideal NRZ-L	± 10 R_B, ± 200 R_B	Mod, PA, 2nd Har Fil	Evaluation of Raised Cosine filter ($\alpha = 0.25$), ideal NRZ-L data.
8	PCM/PM/NRZ	Baseband	Raised Cosine	$\alpha = 0.25$	Non-Ideal NRZ-L	± 10 R_B, ± 200 R_B	Mod, PA, 2nd Har Fil	Evaluation of Raised Cosine filter ($\alpha = 0.25$), non-ideal NRZ-L data.
9	PCM/PM/NRZ	Baseband	Raised Cosine	$\alpha = 0.5$	Ideal NRZ-L	± 10 R_B, ± 200 R_B	Mod, PA, 2nd Har Fil	Evaluation of Raised Cosine filter ($\alpha = 0.5$), ideal NRZ-L data.
10	PCM/PM/NRZ	Baseband	Raised Cosine	$\alpha = 0.5$	Non-Ideal NRZ-L	± 10 R_B, ± 200 R_B	Mod, PA, 2nd Har Fil	Evaluation of Raised Cosine filter ($\alpha = 0.5$), non-ideal NRZ-L data.
11	PCM/PM/NRZ	Baseband	Raised Cosine	$\alpha = 1$	Ideal NRZ-L	± 10 R_B, ± 200 R_B	Mod, PA, 2nd Har Fil	Evaluation of Raised Cosine filter ($\alpha = 1$), ideal NRZ-L data.
12	PCM/PM/NRZ	Baseband	Raised Cosine	$\alpha = 1$	Non-Ideal NRZ-L	± 10 R_B, ± 200 R_B	Mod, PA, 2nd Har Fil	Evaluation of Raised Cosine filter ($\alpha = 1$), non-ideal NRZ-L data.
13	PCM/PM/NRZ	Baseband	Sq Root Raised Cosine	$\alpha = 1$	Ideal NRZ-L	± 10 R_B, ± 200 R_B	Mod, PA, 2nd Har Fil	Evaluation of Square Root Raised Cosine filter ($\alpha = 1$), ideal NRZ-L data.
14	PCM/PM/NRZ	Baseband	Sq Root Raised Cosine	$\alpha = 1$	Non-Ideal NRZ-L	± 10 R_B, ± 200 R_B	Mod, PA, 2nd Har Fil	Evaluation of Square Root Raised Cosine filter ($\alpha = 1$), non-ideal NRZ-L data.
15	PCM/PM/NRZ	Baseband	Raised Cosine	$\alpha = 1$	Ideal Sampled	± 10 R_B, ± 200 R_B	Mod, PA, 2nd Har Fil	Evaluation of Raised Cosine filter ($\alpha = 1$), ideal Sampled data.
16	PCM/PM/NRZ	Baseband	Raised Cosine	$\alpha = 1$	Non-Ideal Sampled	± 10 R_B, ± 200 R_B	Mod, PA, 2nd Har Fil	Evaluation of Raised Cosine filter ($\alpha = 1$), non-ideal Sampled data.
17	PCM/PM/NRZ	Baseband	Sq Root Raised Cosine	$\alpha = 1$	Ideal Sampled	± 10 R_B, ± 200 R_B	Mod, PA, 2nd Har Fil	Evaluation of Square Root Raised Cosine filter ($\alpha = 1$), ideal Sampled data.
18	PCM/PM/NRZ	Baseband	Sq Root Raised Cosine	$\alpha = 1$	Non-Ideal Sampled	± 10 R_B, ± 200 R_B	Mod, PA, 2nd Har Fil	Evaluation of Square Root Raised Cosine filter ($\alpha = 1$), non-ideal Sampled data.

3.0 SIMULATION RESULTS

Simulations were completed for each case listed in Table 2-2. Simulation modeling estimated the performance of actual hardware (non-ideal modulator, multiplier, and power amplifier) using both ideal and non-ideal data sources for all cases. The objective was to ensure that simulation results accurately predicted true hardware performance. Figure 3-1 is a block diagram of the flight system, showing filter locations and alternative study conditions.

For each of the cases listed in Table 2-2, individual spectra were simulated and plotted for: (1) the data source, either the data itself where no filter is present or at the filter's output if one was used, (2) at the output of the power amplifier (prior to the 2^{nd} harmonic filter), and (3) at the output of the 2^{nd} harmonic filter.

Different spectrum widths and resolutions were used depending upon the point being investigated. All spectral frequency axes are labeled in terms of R_B, where R_B is the normalized spectral frequency occupied by a single bit in the telemetry data stream. This generalized labeling permits the reader to scale the results of these simulations to any desired data rate.

At baseband, filtered and unfiltered data spectrum plots have a width of $f_0 \pm 10\ R_B$. The power amplifier's output is also plotted $f_C \pm 10\ R_B$, where f_C is the residual carrier's frequency. These two comparatively high resolution (resolution = 8 Hz) plots permit examination of the transmitted signal's fine structure for accurate determination of the filter's attenuation. A 4^{th} Order Butterworth bandpass filter with a cut-off frequency of $f_C \pm 20\ R_B$, which does not affect the baseband filtering, follows the power amplifier. Its purpose is to simulate a 2^{nd} harmonic filter frequently used following power amplifiers to protect users of other bands. So that a large part of the frequency band will be visible, these plots cover a range of $f_C \pm 200\ R_B$ with a resolution of 11 Hz.

3.1 Reference Data

Simulations were made using unfiltered data (Table 2-2, Case Nos. 1 and 2) to establish a benchmark for comparing the several filter types. Figure 3-2 contains a series of plots for ideal data while Figure 3-3 contains equivalent plots but for non-ideal data. Comparing Figure 3-2a with Figure 3-3a clearly demonstrates the difference in the baseband frequency spectrum for ideal and non-ideal data. Note the significantly increased spurious emissions, including in-band components, present in the non-ideal data.

When unfiltered NRZ-L data is modulated, multiplied and amplified using imperfect system components in a PCM/PM/NRZ format, the results appear in Figures 3-2b and 3-3b. Spurious emissions with in-band components present in the baseband data, also appear at the output of the power amplifier. This spectrum plot represents the power amplifier's output prior to the 2^{nd} harmonic filter so that readers can see the full effect of both baseband and post power amplifier filtering used in subsequent cases.

From Figure 3-3b, it can be seen that the peak level of the third data sideband (e.g., at $f_C \pm 3\ R_B$) is approximately 21 dB below the peak level of the 1st data sideband and the fifth data sideband (e.g., at $f_C \pm 5\ R_B$) is about 25 dB below the peak level of the 1st data sideband. These levels can serve as references for comparing the various filter options. **For a non-ideal data source, the spurious emissions extend well beyond the *Necessary Bandwidth*. Note: while spectra for ideal data is included in this paper, performance comparisons will be made using spectra for non-ideal data because they should better represent actual operating hardware.**

3.2 Filtered Data

Figures 3-2 and 3-3, showing spectra of unfiltered data, can serve as references with which to compare spectra using different types of baseband filters. Because of their large number, only a limited number of plots could be included and discussed in this paper. For the filtered cases, spectra will be provided at the output of: the baseband filter, the power amplifier, and the 2nd harmonic filter. Furthermore, because the unfiltered baseband reference data (Figures 3-2 and 3-3) applies to each of the cases, it will not be repeated for each filter studied. Readers are referred to the corresponding unfiltered case in order to determine the effect of various filter types on the baseband and transmitted spectra.

For purposes of determining filter efficacy, the only meaningful data is the frequency spectrum that is actually transmitted. Accordingly, the transmitted spectra resulting from unfiltered and filtered data must be compared at the power amplifier's output and at the 2nd harmonic filter's output. These data should provide the most accurate estimate of a real flight hardware system's performance. Results of all simulations for the power amplifier's output are summarized in Table 3-1 for filtered and unfiltered, ideal and non-ideal, data. As with the unfiltered data, three plots are provided for each of the filtered cases corresponding to: (1) the baseband filter's output, (2) the power amplifier's output, and (3) the output of the 4th Order Butterworth 2nd harmonic filter with a bandwidth of $\pm 20\ R_B$.

3.2.1 Butterworth Filter, 5th Order

From Table 2-2, the first filter to be considered is the 5th Order Butterworth. The BT product for this filter was set to 1.0 and the bandwidth to R_B. Figures 3-4 and 3-5 depict system's performance using this filter for ideal and non-ideal NRZ-L data respectively. Figures 3-4a and 3-5a should be compared to Figures 3-2a and 3-3a for the ideal and non- ideal data cases respectively. At $\pm 2\ R_B$, the filter attenuates the baseband data sidebands by 40 dB, using a non-ideal data source. However, note the ringing at the knee of the curve, which is probably the result of the filter's high (5th) Order. The effect of this ringing will become apparent as the signal passes through additional non-linear elements.

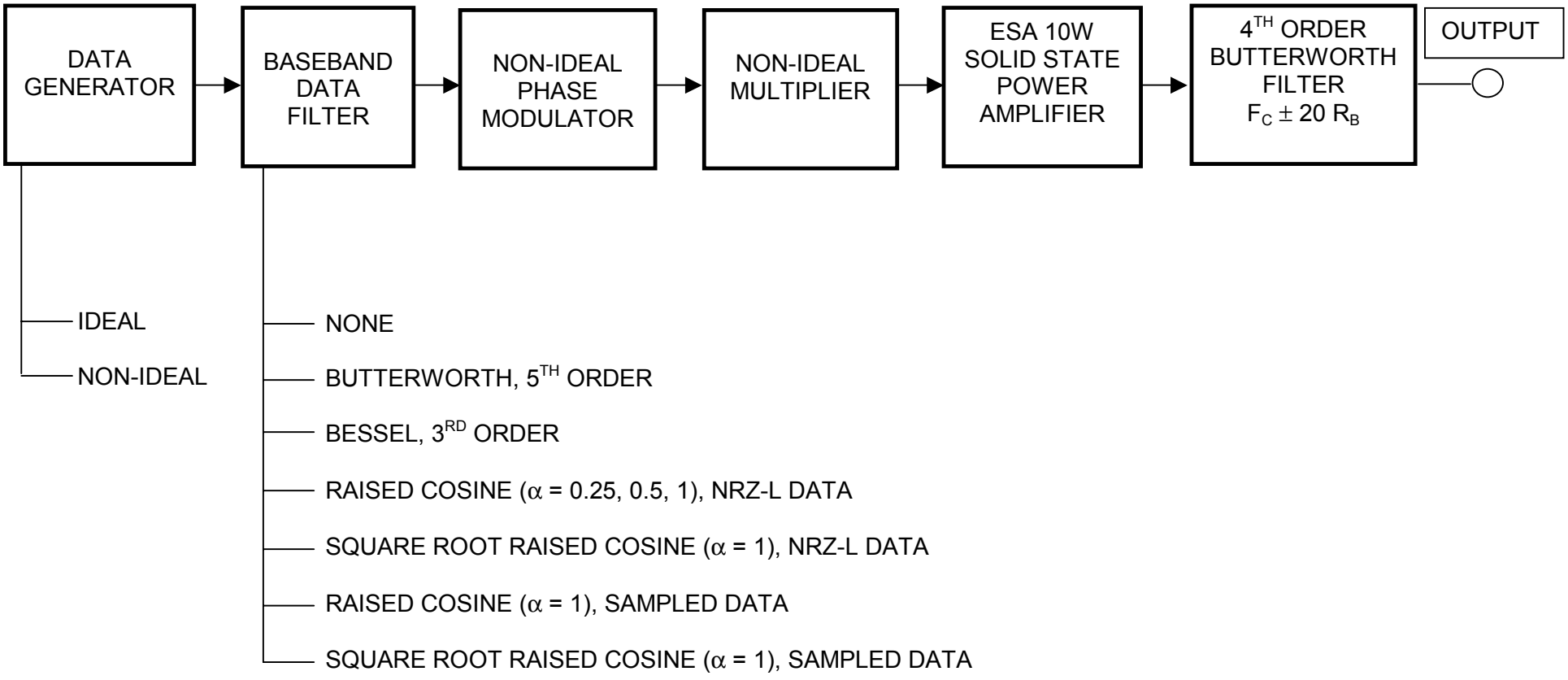

Figure 3-1. Spacecraft Configuration for Evaluating Alternative Modulation Methods

Figures 3-4b and 3-5b show the spectrum at the power amplifier's output. Note the spurious emissions, with in-band components, at frequency intervals of R_B which probably result from filter ringing, non-ideal components, and perhaps the ISI. The large spurious signals are present for both ideal and non-ideal data but additional, lower level spurious emissions can be seen in the frequency spectrum using non-ideal data. Figures 3-4b and 3-5b should be compared with Figures 3-2b and 3-3b respectively. Spurious emissions, with in-band components, are very evident in Figure 3-3b where no baseband filtering was used and are clearly the result of non-ideal data. Thus, both the Butterworth baseband filter and non-ideal data are seen to introduce in-band spurious emissions which represent non-recoverable data power. **However, comparing Figures 3-3b and 3-5b reveals that the filtering significantly reduces the spurious emission level.**

Figures 3-4c and 3-5c are the frequency spectra at the output of the 4^{th} Order Butterworth 2^{nd} harmonic bandpass filter which follows the power amplifier. Initially, this filter had a cut-off frequency of $f_C \pm 150\ R_S$ and was intended to reduce the second harmonic emission. However, the non-linear transmitting system produced both odd and even harmonics with the result that significant emissions are present at $f_C \pm 50\ R_B$, $\pm 100\ R_B$, etc. Therefore, these simulations used a second harmonic filter bandwidth of $f_C \pm 20\ R_B$.

From a Frequency Manager's perspective, the important result from baseband filtering can be seen when comparing Figures 3-3c and 3-5c. At $f_C \pm 5\ R_B$, the Butterworth filter attenuates the sidebands by an additional 22 dB, placing the absolute level of sidebands beyond $\pm 5\ R_B$ at 47 dB, or more, below the peak of the main data lobe. Whether this additional attenuation is sufficient to greatly increase band utilization is discussed in Section 5. A summary of the attenuation provided by each filter type will be found in Table 3-1.

The in-band spurious emissions are a cause of concern for Butterworth filters. Initially, it was thought that these spurious signals could be the result of Inter-Symbol Interference (ISI). To investigate this possibility, the Butterworth filter's bandwidth was widened from approximately 1 R_B to about 5 R_B. The result was a reduction in the amplitude of the in-band spurious signal near the carrier but an increase in these same emissions at and around $\pm 5\ R_B$. No significant benefit was obtained by widening the Butterworth filter's bandwidth.

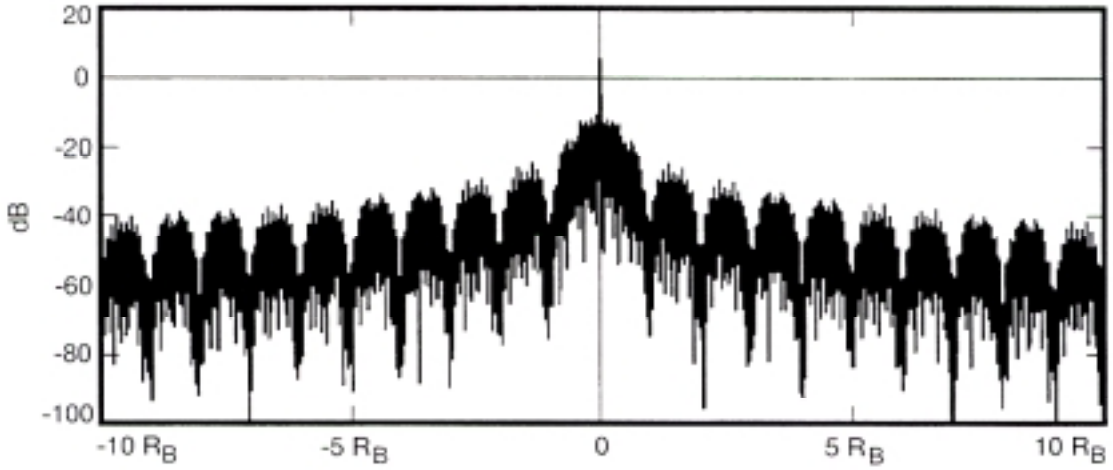

Figure 3-2a. Unfiltered Baseband Data

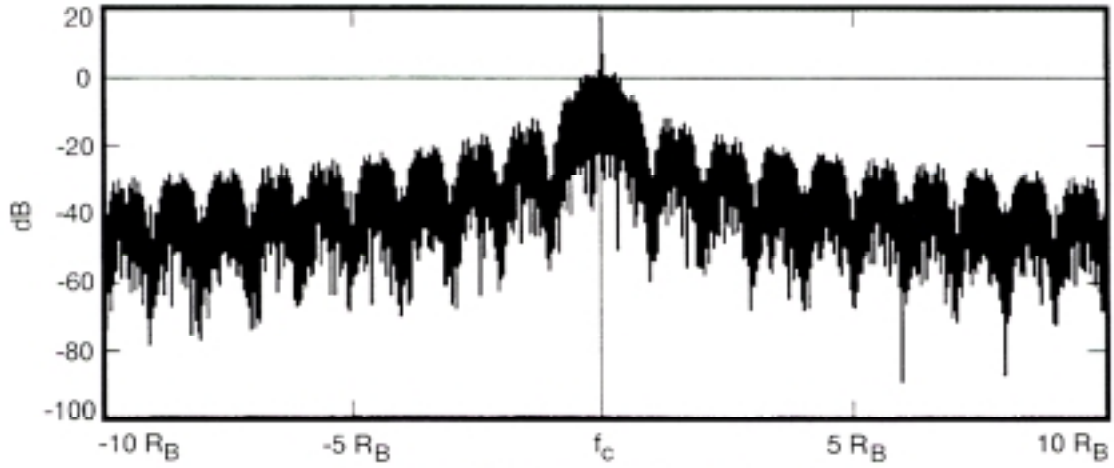

Figure 3-2b. Output of Power Amplifier

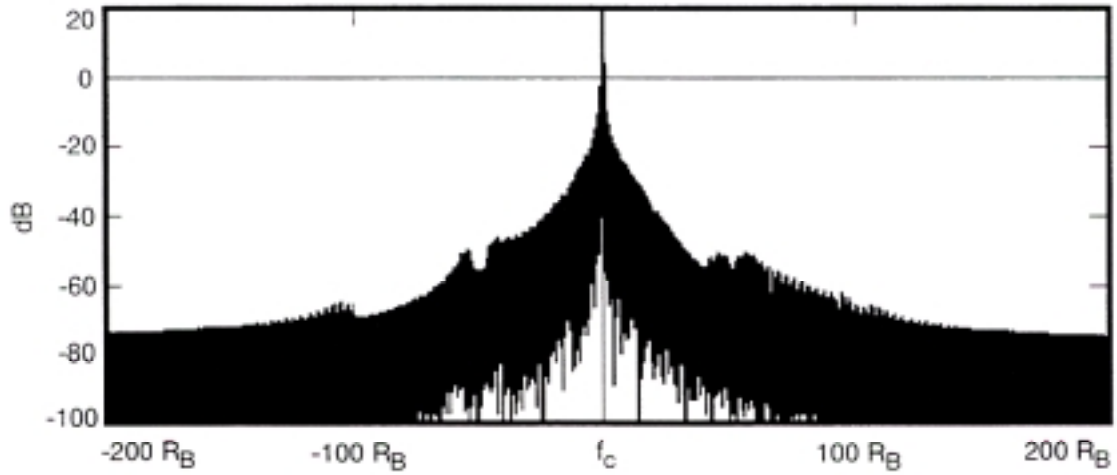

Figure 3-2c. Output of Second Harmonic Filter (± 20 R_B)

Figure 3-2. Unfiltered Baseband NRZ=L Data Spectra (Ideal Data)

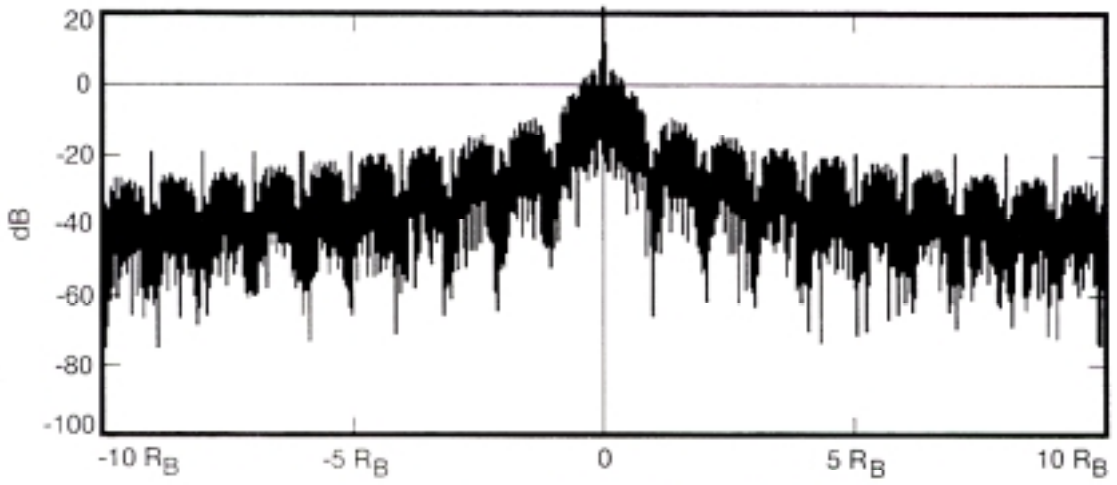

Figure 3-3a. Unfiltered Baseband Data

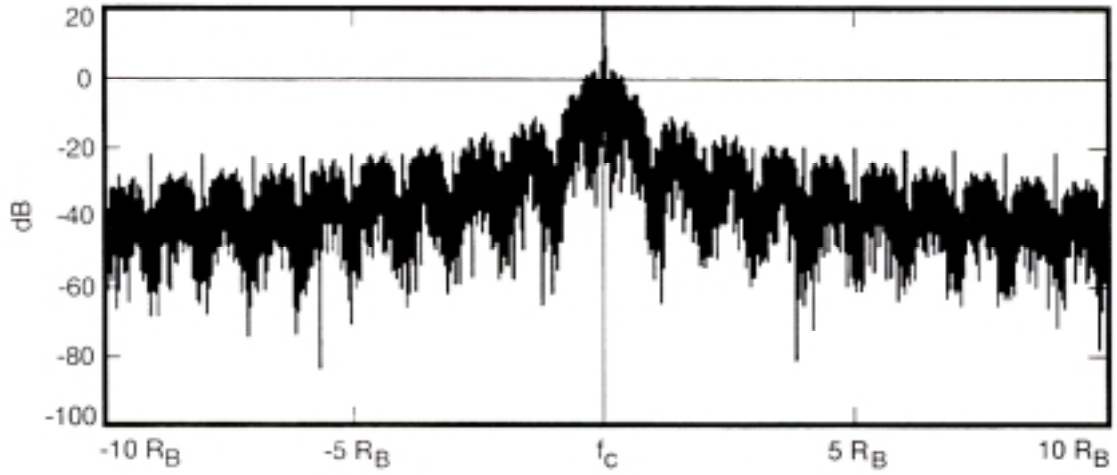

Figure 3-3b. Output of Power Amplifier

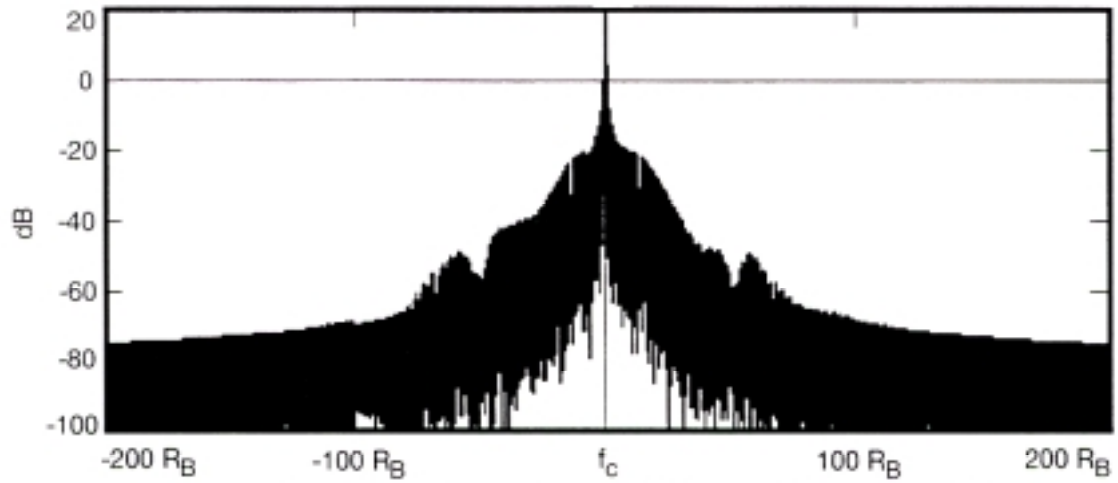

Figure 3-3c. Output of Second Harmonic Filter (± 20 R_B)

Figure 3-3. Unfiltered Baseband NRZ-L Data Spectra (Non-Ideal Data)

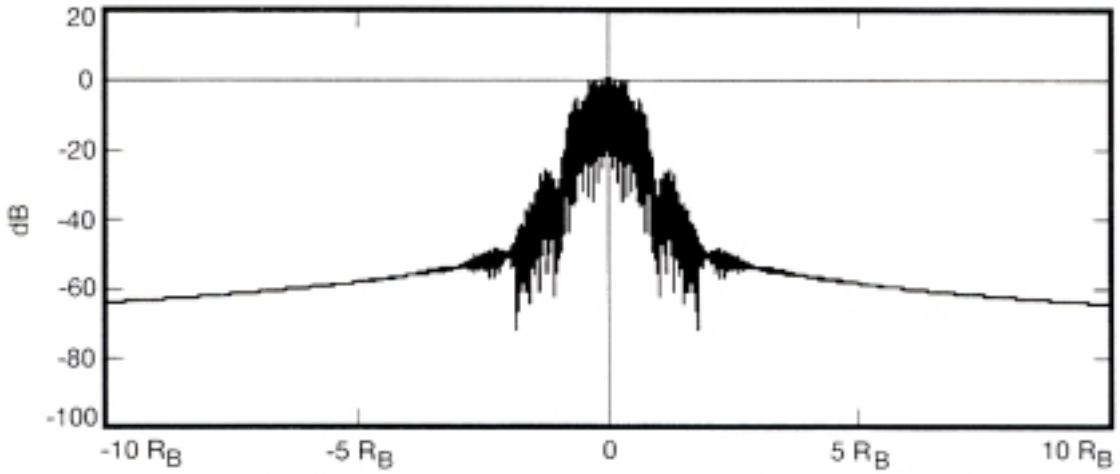

Figure 3-4a. Output from Butterworth Filter (5th Order)

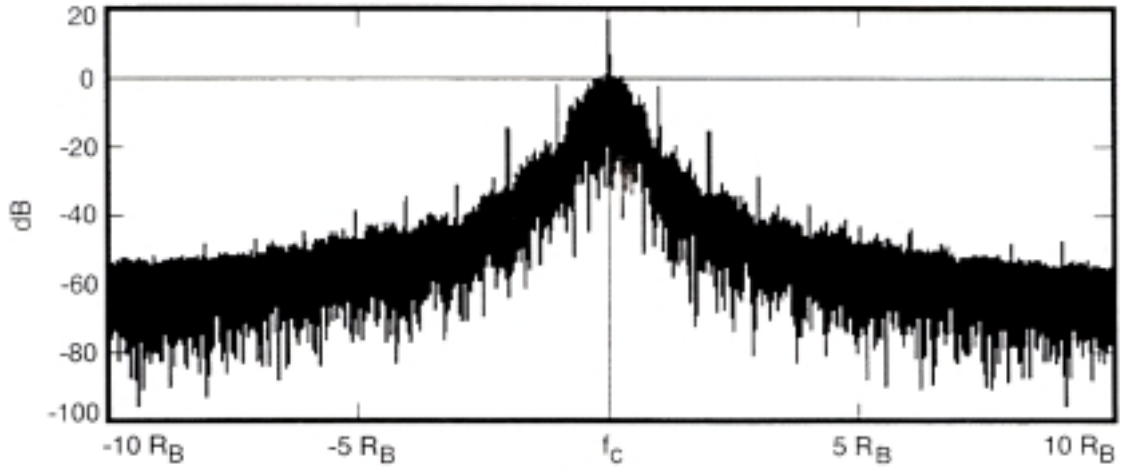

Figure 3-4b. Output of Power Amplifier

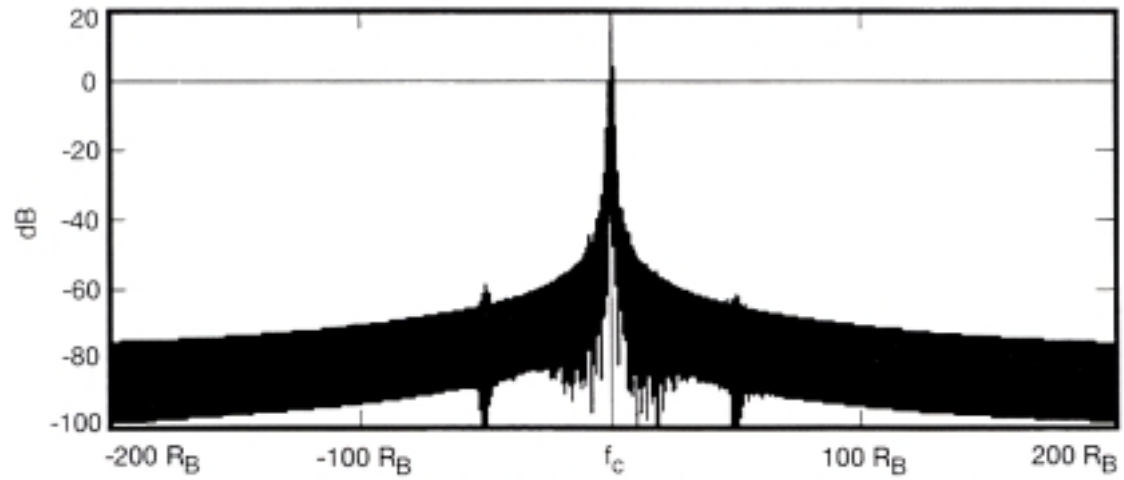

Figure 3-4c. Output of Second Harmonic Filter (± 20 R_B)

Figure 3-4. Baseband 5th Order Butterworth Filtered NRZ-L Data Spectra (Ideal Data)

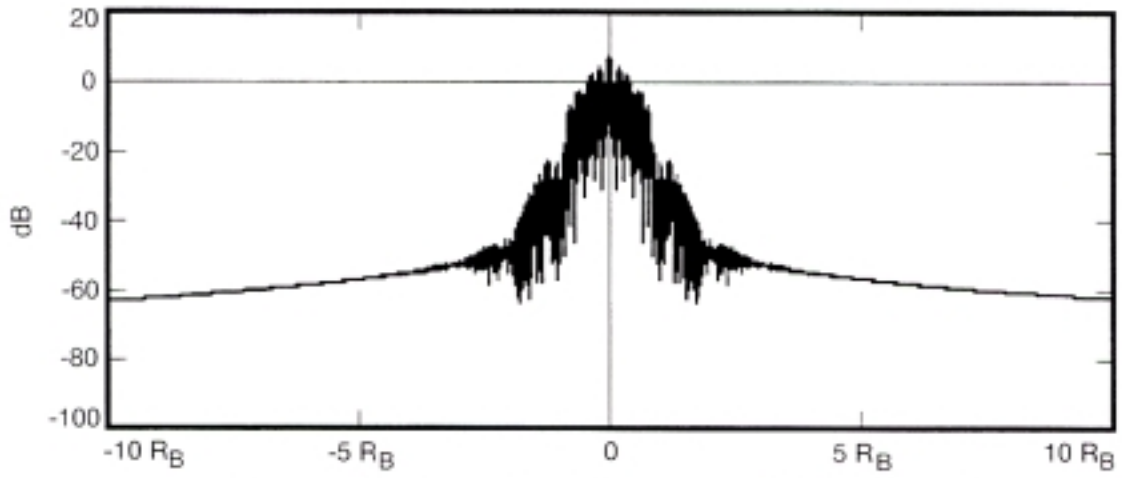

Figure 3-5a. Output from Butterworth Filter (5th Order)

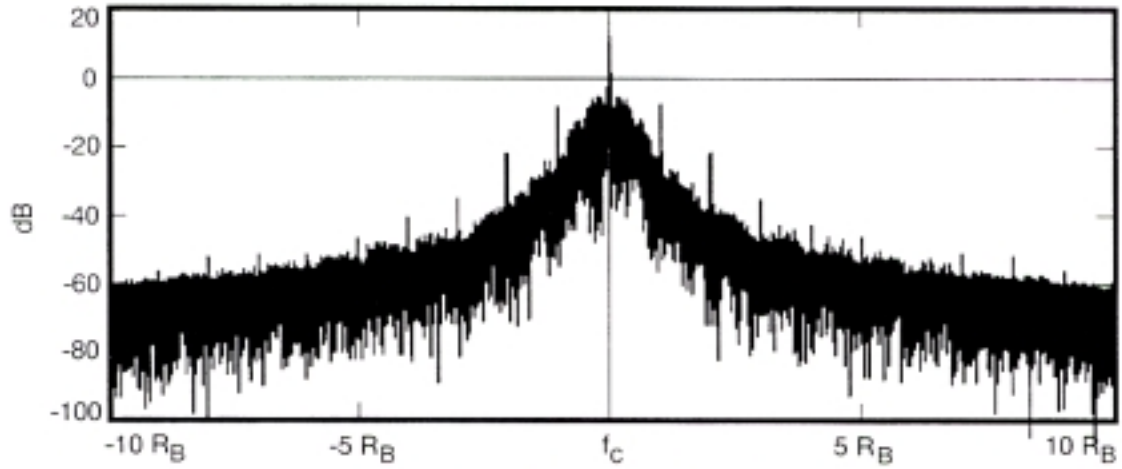

Figure 3-5b. Output of Power Amplifier

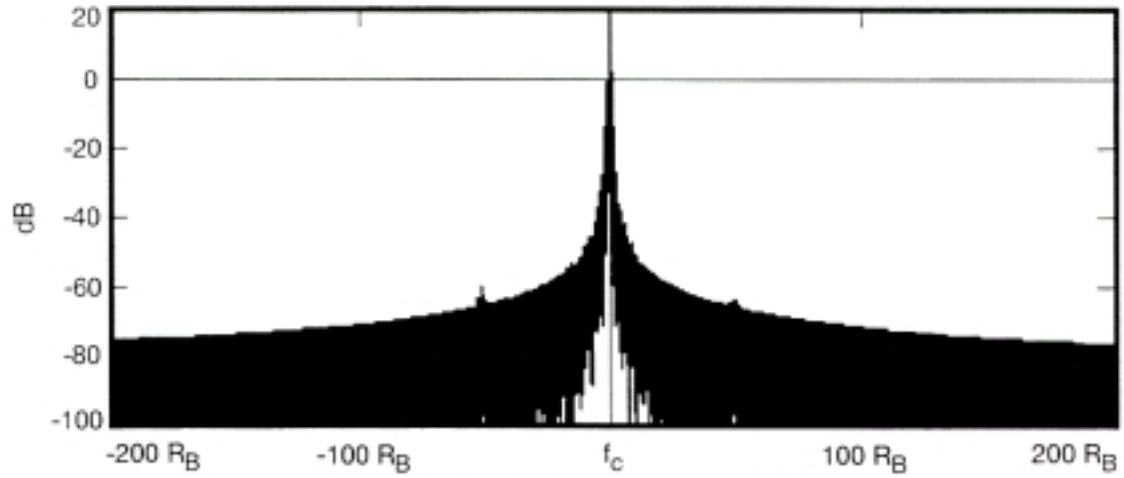

Figure 3-5c. Output of Second Harmonic Filter (± 20 R_B)

Figure 3-5. Baseband 5th Order Butterworth Filtered NRZ-L Data Spectra (Non-Ideal Data)

3.2.2 Bessel Filter

A 3rd Order Bessel filter is an alternative to the Butterworth filter. For consistency, a BT product of 1.0 and a bandwidth of R_B were selected. Some writers suggest that Bessel filters are superior to Butterworth filters when applied to baseband signals. Spectra for this filter appear in Figures 3-6 and 3- 7 and should be compared with Figures 3-4 and 3-5 respectively.

Comparing Figures 3-5b and 3- 7b (power amplifier outputs) reveals that the modulated and amplified spectra are virtually identical for the two filters. Both exhibit a significant number of in-band spurious emissions. Likewise, comparing Figures 3-5c and 3- 7c (2nd harmonic filter output) shows that the transmitted spectra are substantially indistinguishable from one another. Attenuation values contained in Table 3-1 show the Butterworth filter to be superior. The Bessel filter's poorer attenuation is probably due to its comparatively low Order. Like Butterworth filters, there is some concern regarding the use of Bessel filters because of the in-band spurious emissions.

3.2.3 Raised Cosine Filters

Raised Cosine filters were selected for evaluation because the linearity of their phase-frequency relationship should help to eliminate the ringing found in Butterworth filters at the cut-off frequency. Their comparatively narrow bandwidth, combined with a smooth response, should provide a signal which concentrates most of the data sideband energy in or near the main lobe significantly attenuating the sidebands. Such filters are commonly employed to pack a multiplicity of signals in a confined frequency band.

Raised Cosine filters accept two types of input signals: non-sampled and sampled. With non-sampled input signals like NRZ-L, d(t), the Raised Cosine filter behaves in a manner similar to a passive filter with a transfer function, X(f), having a Raised Cosine shape (Reference 10). Here, the filter's output is the convolution of the input signal d(t) with x(t) where x(t) is the inverse Fourier transform of X(t). Conversely, when the input signal is sampled (e.g., a pulse of short duration with an amplitude of + 1 representing a "1" and a similar pulse of short duration with an amplitude of -1 representing a "0"), the Raised Cosine filter acts like a waveform generator producing a true Raised Cosine shape of X(f) in the frequency domain. In practice, one can obtain a Raised Cosine waveform using a non-Sampled data input by cascading the Raised Cosine filter and a 1/Sinc filter. Note that Sinc(t) is defined as sin(t)/t.

Maximizing data transmission efficiency requires the receiver have a filter matching the one at the transmitter. For linear channels (e.g., channels without AM-AM and AM-PM conversions), placing a Raised Cosine or Square Root Raised Cosine filter at the transmitter requires installing the same filter at the receiver. The result is a system transfer function approximating a [Raised Cosine]^2 or a Raised Cosine function respectively. With this implementation, one can obtain ISI-free sample points for optimum data detection (see Figures 4-2a and 4-2c).

However, for non-linear channels, such as those considered here, the principle is no longer applicable because of the distortion introduced by the system. With such channels, ISI-free sample points no longer exist as shown in Figures 4-2b and 4-2d. The objective of this study is not only to find a bandwidth efficient communications system which can increase frequency band utilization, but also, to identify an implementation that can be realized. Accordingly, detection and ISI will be discussed in greater detail in Section 4.

The "bandwidth" of a Raised Cosine filter is determined by a parameter termed a which can be varied from 0 to 1. For $\alpha = 0$, the filter's transfer function approximates that of a "Brick Wall" filter with bandwidth T while an $\alpha = 1$ yields a sinusoidal transfer function having a total width of 2T. Figure 3-8a depicts the amplitude responses in the frequency domain for a Raised Cosine filter while Figure 3-8b does the same of a Square Root Raised Cosine filter.

As described above, if Sampled data is fed to a Raised Cosine filter, the resulting waveform will be a pure Raised Cosine function rather than the convolution of the inverse Fourier transform with an NRZ-L function. To generate a true Raised Cosine waveform, a Sampled data input rather than a NRZ-L data input is required. Sampled data is produced by generating a pulse, of short duration, having a + 1 amplitude representing each "1" and a pulse of the same duration but having a - 1 amplitude to representing each "0".

To determine if the filter's performance is significantly affected, spectra for both NRZ-L and Sampled data are analyzed. A Sampled data waveform requires modifications to existing spacecraft hardware. However, if the bandwidth reduction resulting from this data type is large, then such alterations may be desirable and worth the expenditure.

In the following sections, spectra for both Raised Cosine and Square Root Raised Cosine filters with NRZ-L and Sampled data inputs are provided. Both filter types have advantages and disadvantages with respect to each other as well as with regard to Butterworth and Bessel filters which can only be illuminated by comparing the several types. To make this comparison it is necessary to examine the transmitted spectra for the several Raised Cosine and Square Root Raised Cosine filters. Spectra for Raised Cosine filters with an NRZ-L input and $\alpha = 0.25$, 0.5, and 1 are provided to demonstrate the effect of this parameter. However, Raised Cosine filters for Sampled data and all Square Root Raised Cosine filters are only evaluated at $\alpha = 1$.

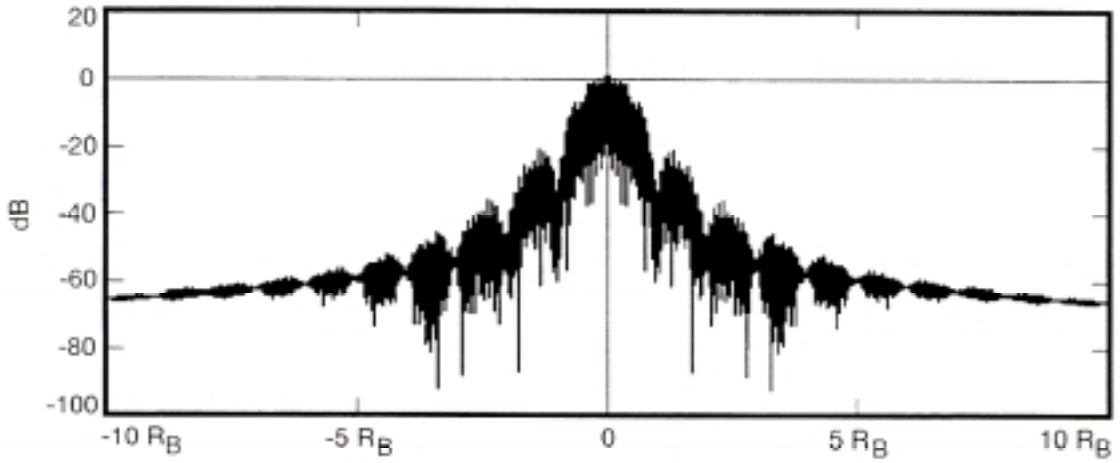

Figure 3-6a. Output from Bessel Filter (3rd Order)

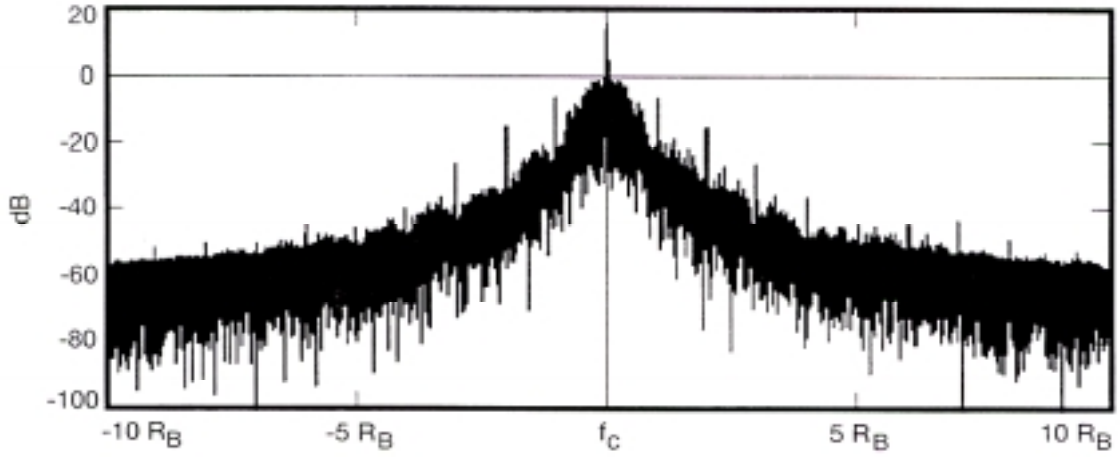

Figure 3-6b. Output of Power Amplifier

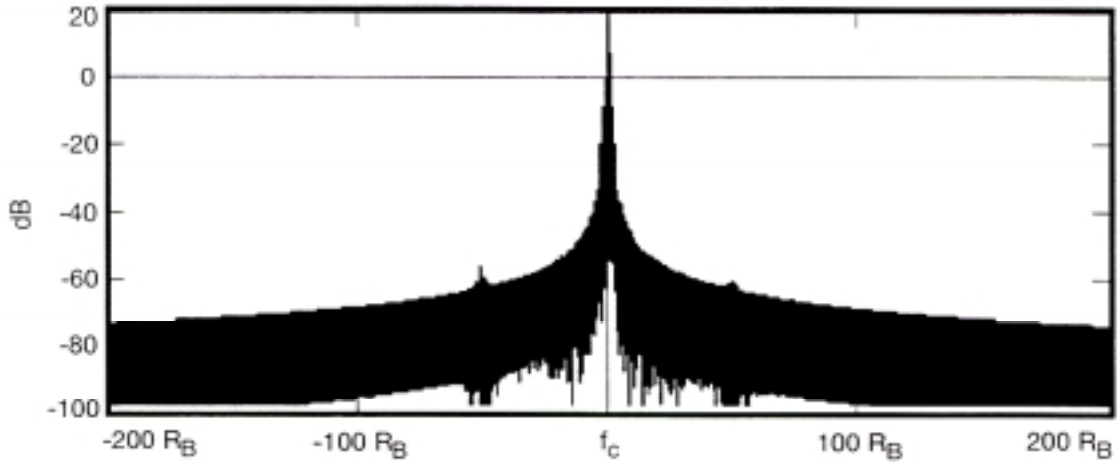

Figure 3-6c. Output of Second Harmonic Filter (± 20 R_B)

Figure 3-6. Baseband 3rd Order Bessel Filtered NRZ-L Data Spectra (Ideal Data)

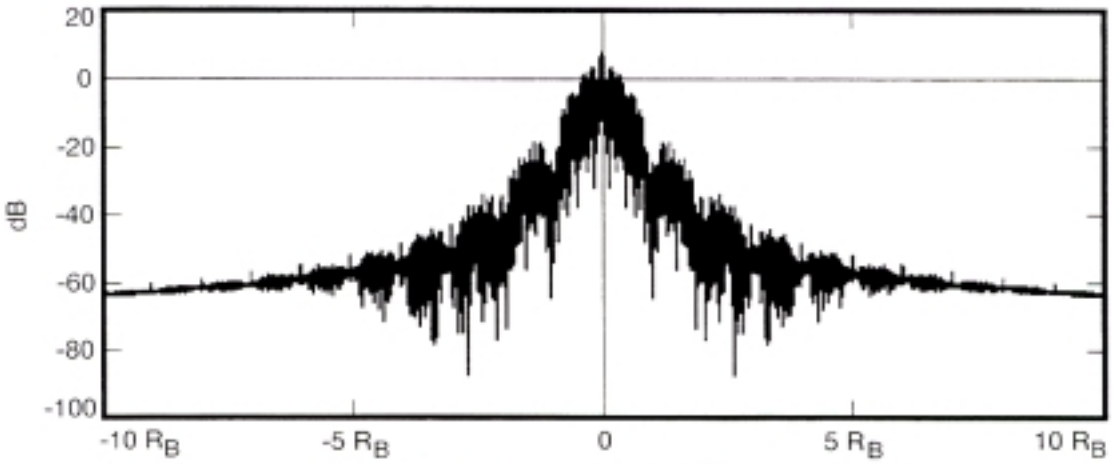

Figure 3-7a. Output from Bessel Filter (3rd Order)

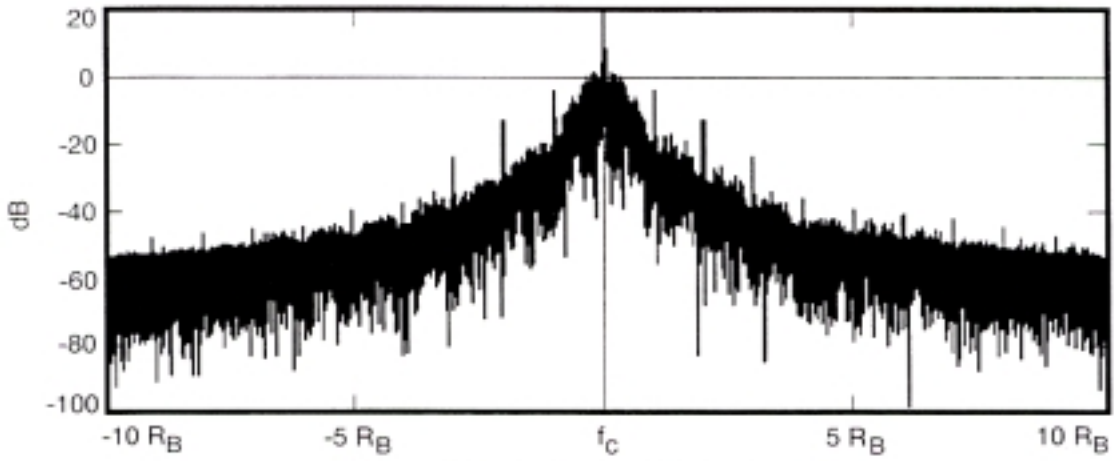

Figure 3-7b. Output of Power Amplifier

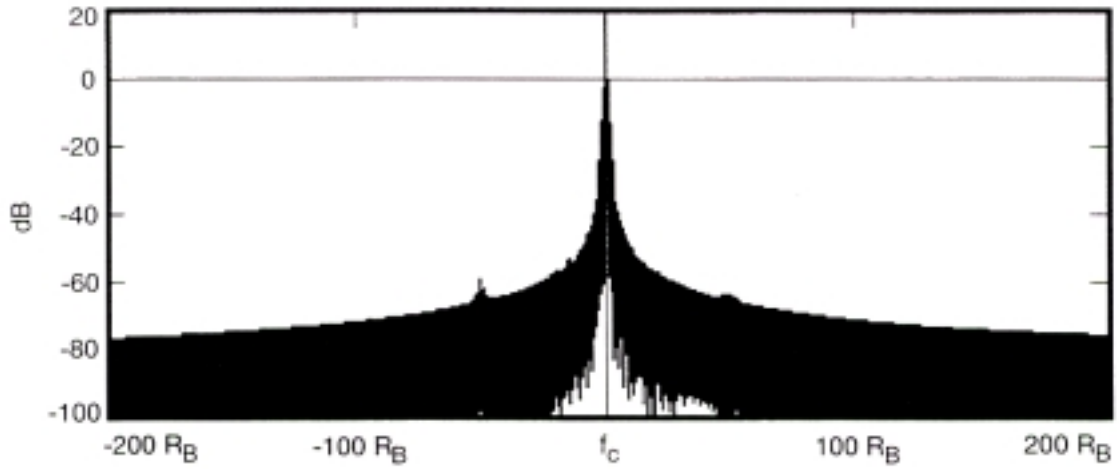

Figure 3-7c. Output of Second Harmonic Filter (± 20 R_B)

Figure 3-7. Baseband 3rd Order Bessel Filtered NRZ-L Data Spectra (Non-Ideal Data)

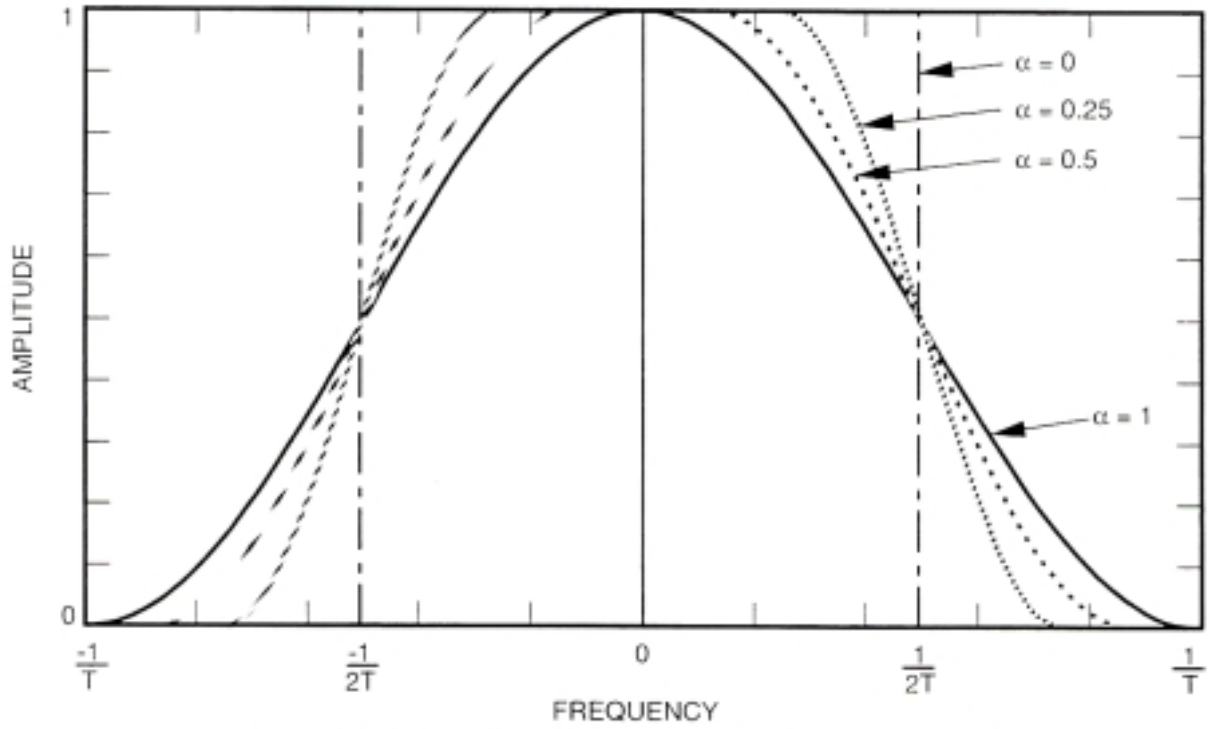

Figure 3-8a. Amplitude Response of a Raised Cosine Filter

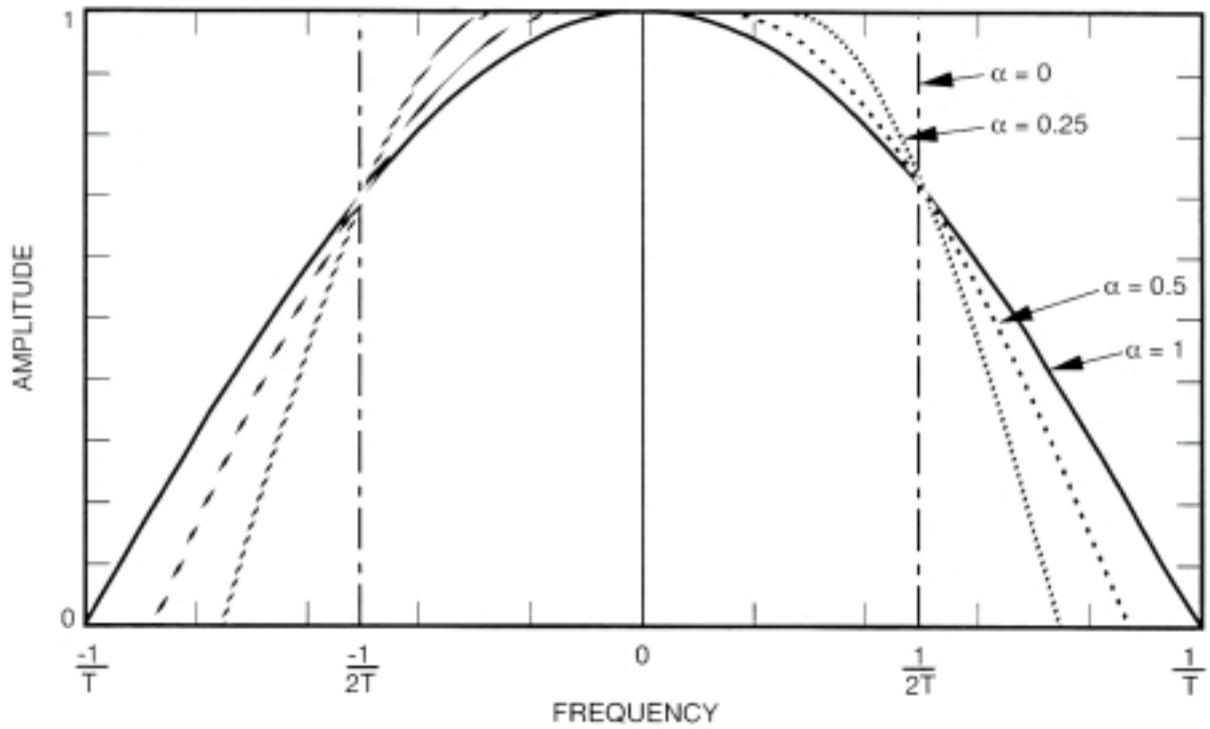

Figure 3-8b. Amplitude Response of a Square Rot Raised Cosine Filter

Figure 3-8. Amplitude Responses for Raised Cosine Filters

3.2.3.1 Raised Cosine Filter (α = 0.25), NRZ-L Data

Comparing Figures 3-9a and 3-10a for a Raised Cosine (α = 0.25) filter with Figures 3-4a and 3-5a for Butterworth and Figures 3-6a and 3- 7a for Bessel filters shows that the former offers a significant advantage over both of the latter filter types. Despite some evidence of higher order sidebands, the spectrum is narrower, cleaner, better defined, than the spectra for other filter types. Moreover, the attenuation at $\pm$ 5 R_B is significantly greater than that for the Butterworth or Bessel filters. In-band spurious emissions are absent, even for non-ideal data. The reason why Raised Cosine filters are frequently chosen to separate signal sources operating in the same band is clearly obvious from Figures 3-9a and 3-10a. With α = 0.25, this is the narrowest bandwidth Raised Cosine filter to be considered in this study.

Outputs from the power amplifier are also comparatively uniform although the greatly attenuated higher order data sidebands are clearly visible in Figures 3-9b and 3-10b for ideal and non-ideal data respectively. Unfortunately, the nonlinearities of the modulator, multiplier, and power amplifier cause a significant increase in amplitude in the 2 to 7 R_B region. Nevertheless, with non-ideal data, the transmitted signal levels are 40 dB below the main lobe at $\pm$ 3 R_B and 53 dB below the main lobe at $\pm$ 5 R_B.

3.2.3.2 Raised Cosine Filter (α = 0.5), NRZ-L Data

Similar RF frequency spectrum levels, using non-ideal data, are found with a Raised Cosine (α = 0.5) filter (Figure 3-12b). This filter provides a transmitted data spectrum which is 43 dB below the main data lobe at $\pm$ 3 R_B and 52 dB below the main lobe at $\pm$ 5 R_B.

As with the previous filter, the transmitted RF spectrum (Figure 3-12c) is comparatively smooth and free of in-band spurious emissions, even for non-ideal data. Since there appears to be no significant difference in the spectra using the two filters, the selection must depend upon other factors such as ISI, implementation complexity, etc.

3.2.3.3 Raised Cosine Filter (α = 1), NRZ-L Data

Because a Raised Cosine filter with an α = 1 has a larger bandwidth than filters with smaller values of α, the baseband data spectrum using non-ideal data (Figure 3-14a) is wider than those described above. However, the higher order data sidebands seen in the previous cases are clearly absent.

At the power amplifier's output (Figure 3-15b), the spectrum is characterized by a smooth roll-off with no in-band spurious emissions evident. Due to this filter's wider bandwidth, the attenuation at $\pm$ 5 R_B is slightly less that for filters with

smaller values of a. At $\pm$ 5 R_B the signal level is 51 dB below the main lobe rather than 52 or 53 dB.

3.2.3.4 Square Root Raised Cosine Filter (α = 1), NRZ-L Data

To obtain two ISI-free sample points, a Square Root Raised Cosine filter was evaluated. Only a single filter with α = 1 was analyzed. Results are shown in Figures 3-15 and 3-16 for ideal and non-ideal data respectively. Like the full Raised Cosine filters, the Square Root Raised Cosine filter was supplied with NRZ-L data.

Figures 3-16b and 3-16c, for the power amplifier and second harmonic filter outputs respectively, also show a smooth roll-off and no spurious emissions, even using non-ideal data. Excellent attenuation was obtained with the signal level at $\pm$ 5 R_B falling to 53 dB below the level of the main data lobe. This is better performance than was obtained with any of the full Raised Cosine, Butterworth, or Bessel filters. The Square Root Raised Cosine filter appears to be a strong candidate for the optimum baseband filter type.

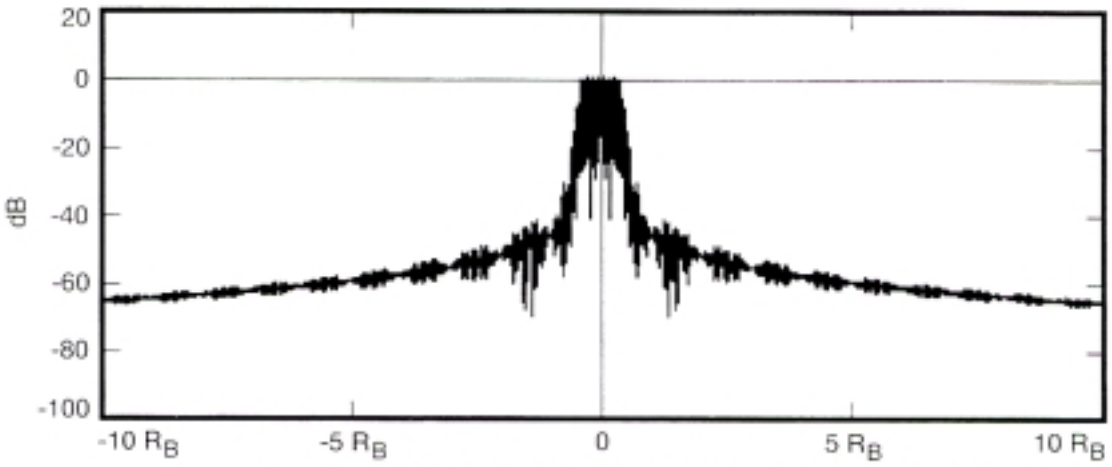

Figure 3-9a. Output from Raised Cosine Filter (α = 0.25; 2000 Taps)

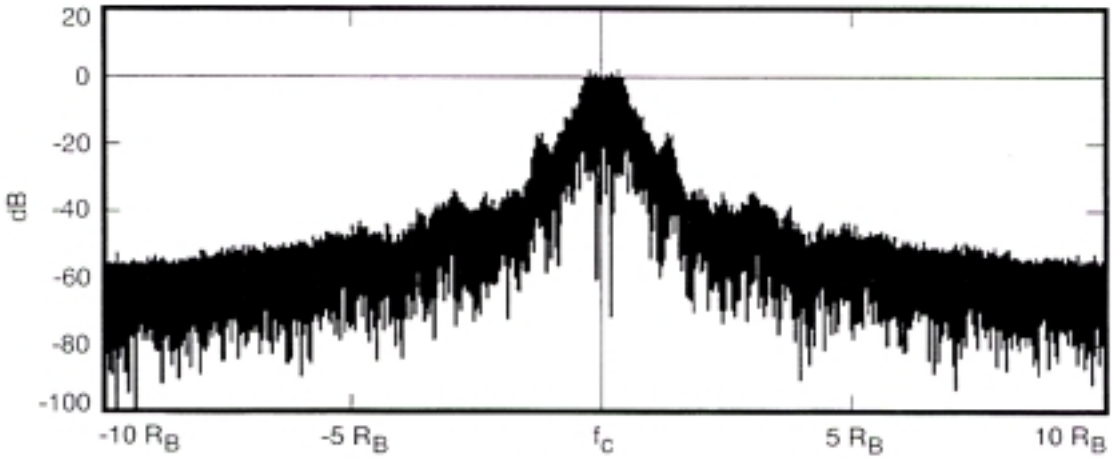

Figure 3-9b. Output of Power Amplifier

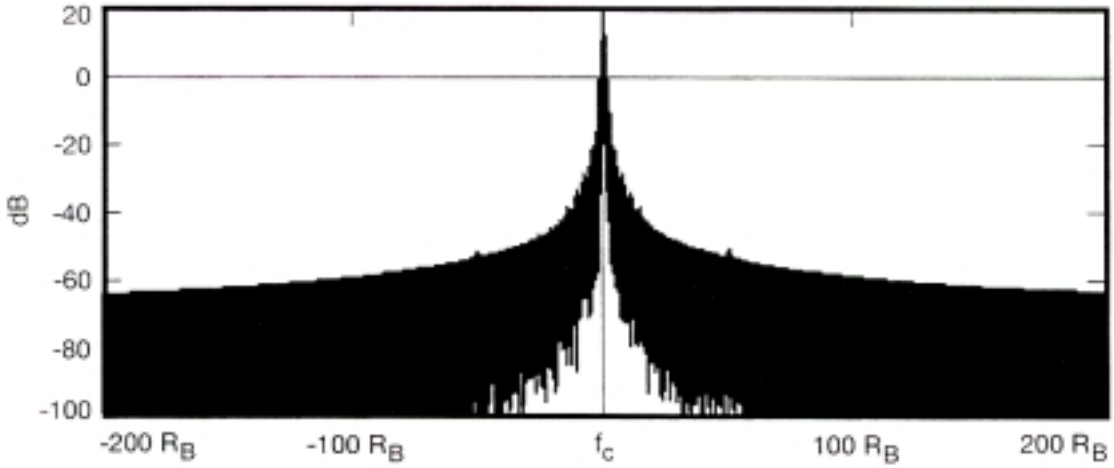

Figure 3-9c. Output of Second Harmonic Filter (± 20 R_B)

Figure 3-9. Baseband Raised Cosine Filtered NRZ-L Data Spectra, α = 0.25 (Ideal Data)

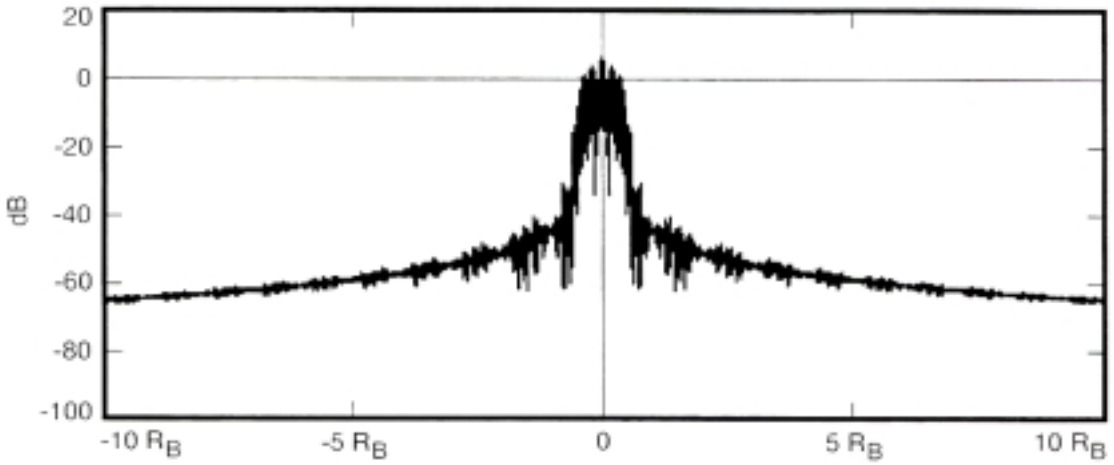

Figure 3-10a. Output from Raised Cosine Filter (α = 0.25; 2000 Taps)

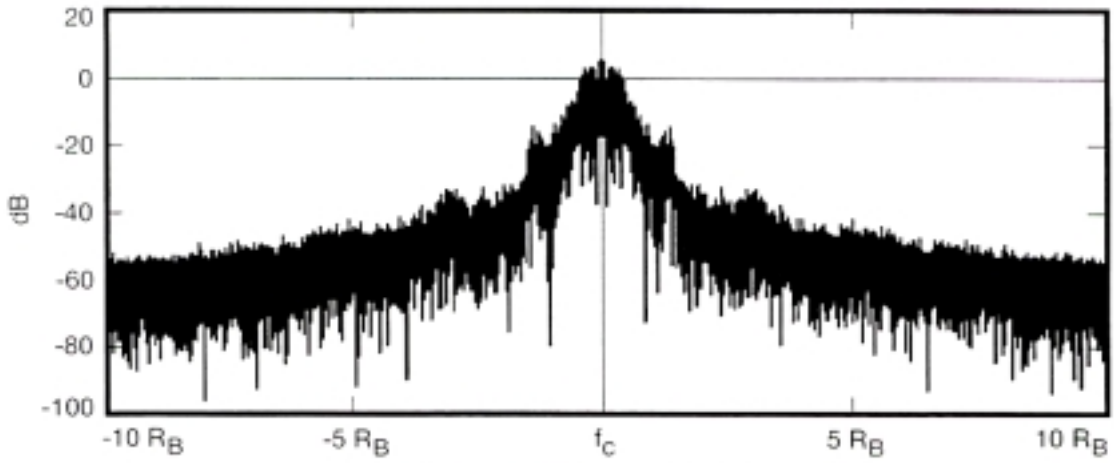

Figure 3-10b. Output of Power Amplifier

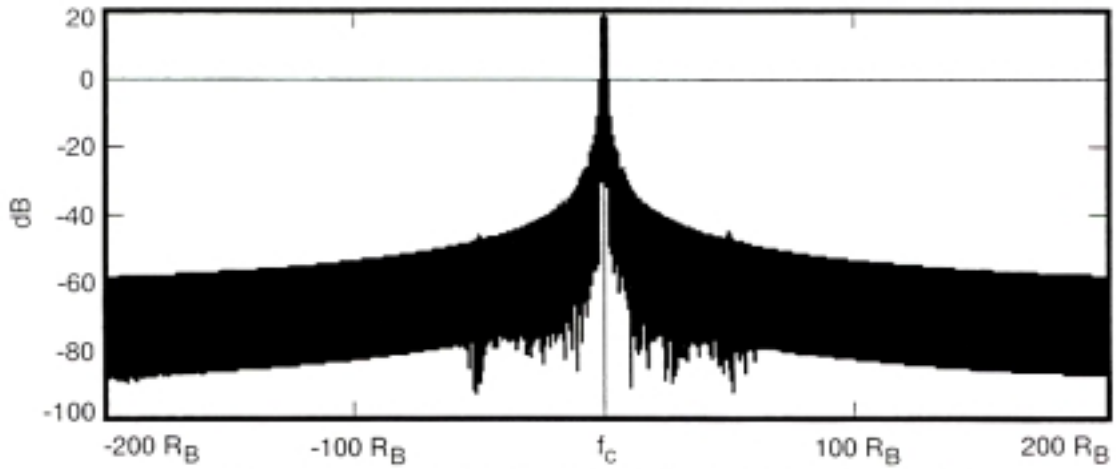

Figure 3-10c. Output of Second Harmonic Filter (± 20 R_B)

Figure 3-10. Baseband Raised Cosine Filtered NRZ-L Data Spectra, α = 0.25 (Non-Ideal Data)

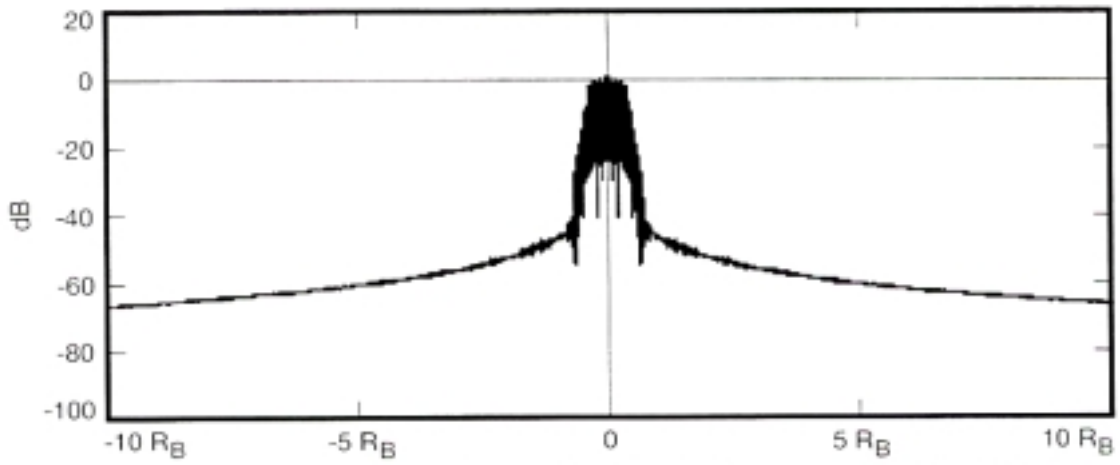

Figure 3-11a. Output from Raised Cosine Filter (α = 0.5; 2000 Taps)

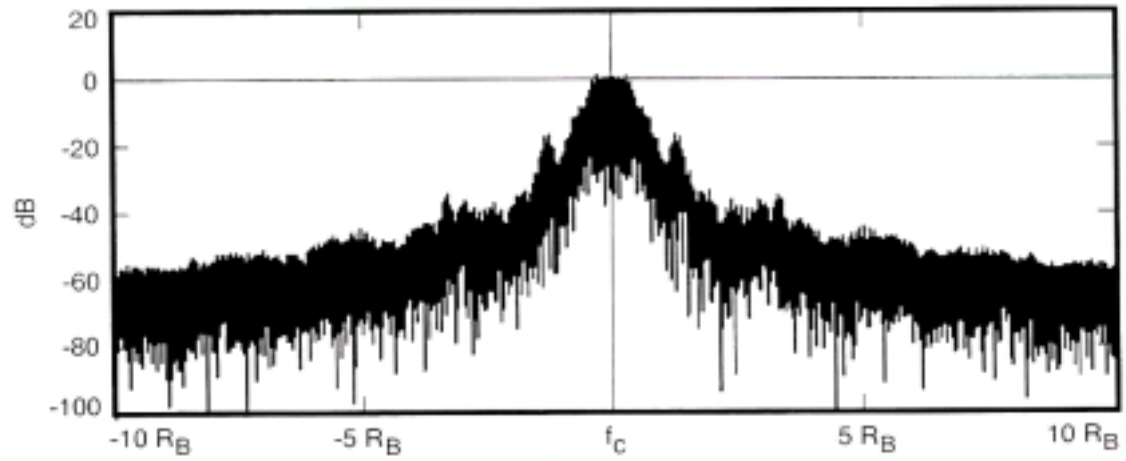

Figure 3-11b. Output of Power Amplifier

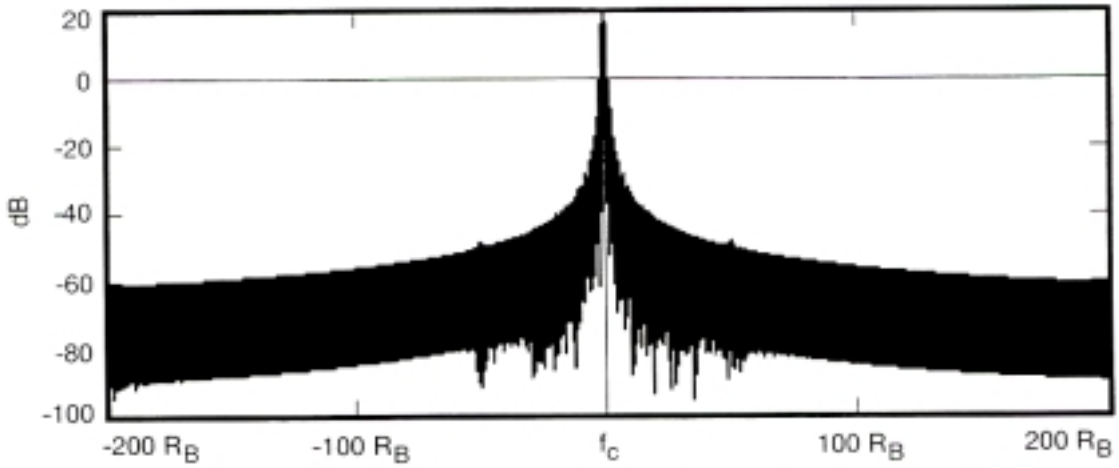

Figure 3-11c. Output of Second Harmonic Filter ($\pm$ 20 R_B)

Figure 3-11. Baseband Raised Cosine Filtered NRZ-L Data Spectra, α = 0.5 (Ideal Data)

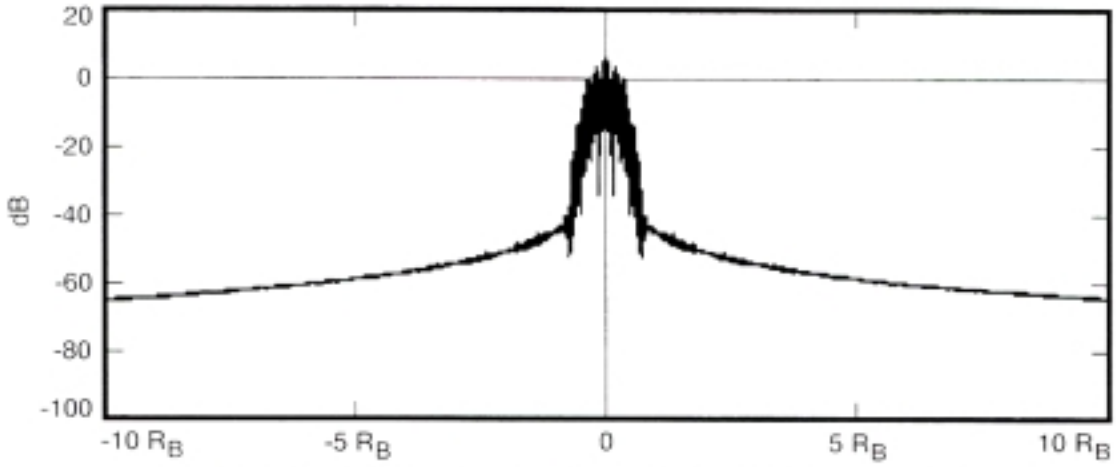

Figure 3-12a. Output from Raised Cosine Filter (α = 0.5; 2000 Taps)

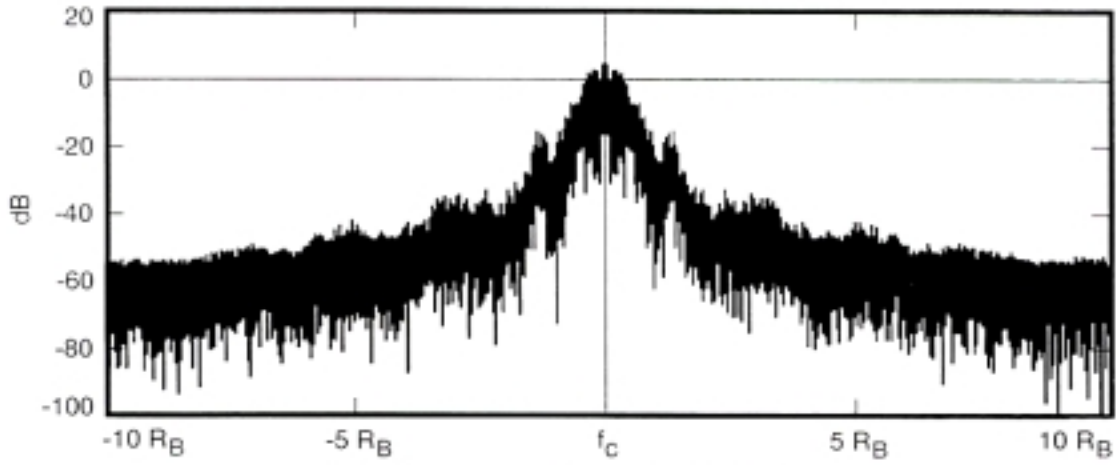

Figure 3-12b. Output of Power Amplifier

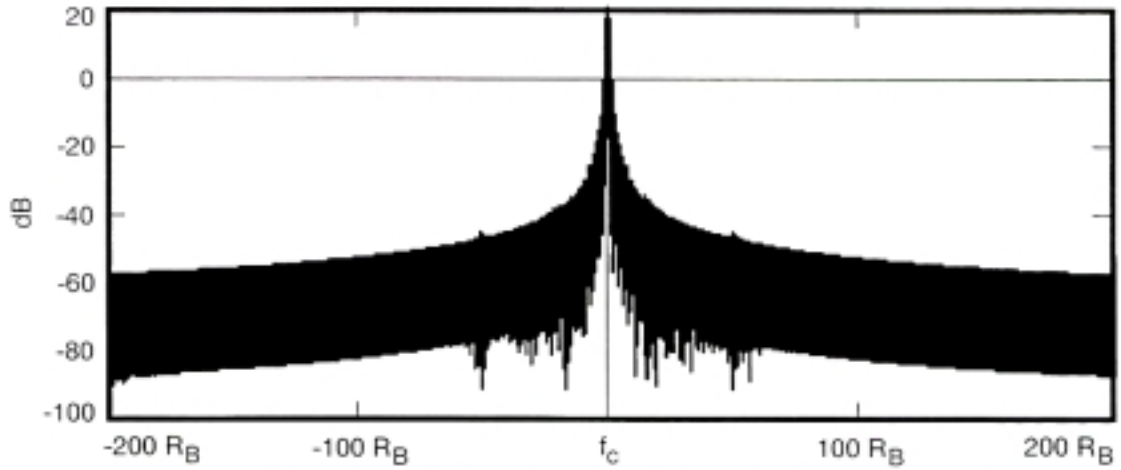

Figure 3-12c. Output of Second Harmonic Filter (± 20 R_B)

Figure 3-12. Baseband Raised Cosine Filtered NRZ-L Data Spectra, α = 0.5 (Non-Ideal Data)

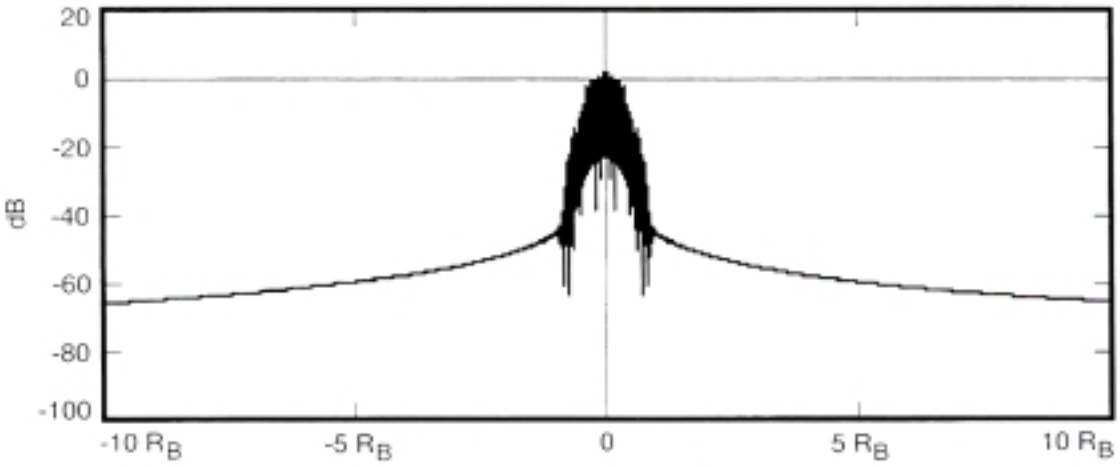

Figure 3-13a. Output from Raised Cosine Filter (α = 1; 2000 Taps)

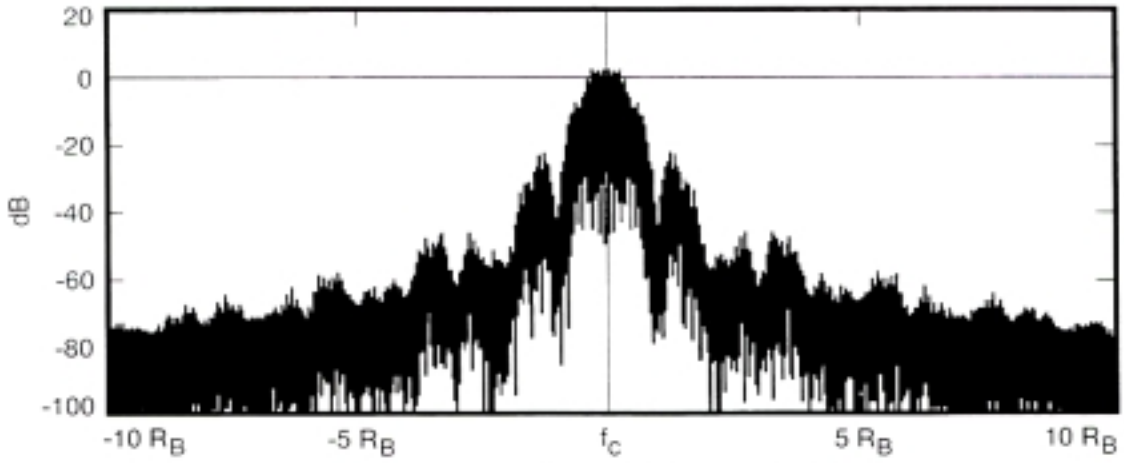

Figure 3-13b. Output of Power Amplifier

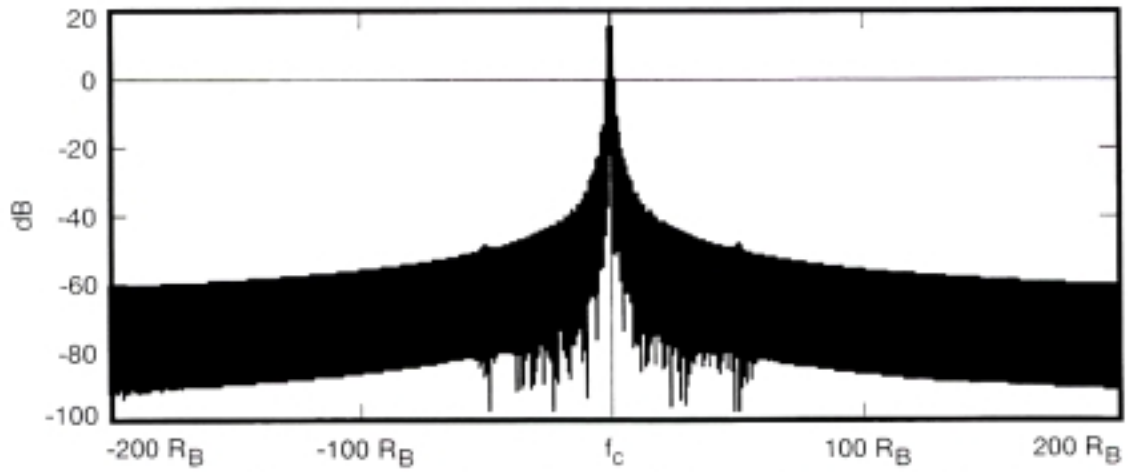

Figure 3-13c. Output of Second Harmonic Filter (± 20 R_B)

Figure 3-13. Baseband Raised Cosine Filtered NRZ-L Data Spectra, α = 1 (Ideal Data)

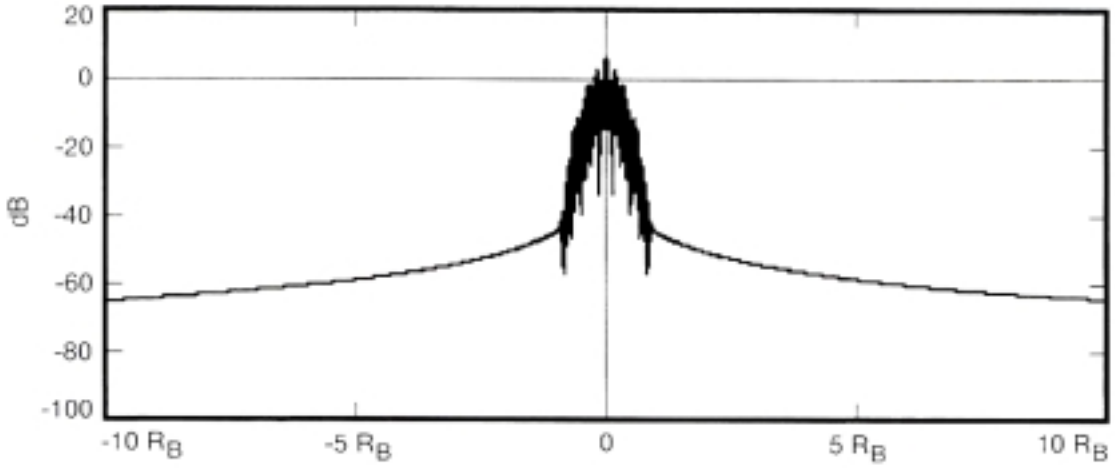

Figure 3-14a. Output from Raised Cosine Filter (α = 1; 2000 Taps)

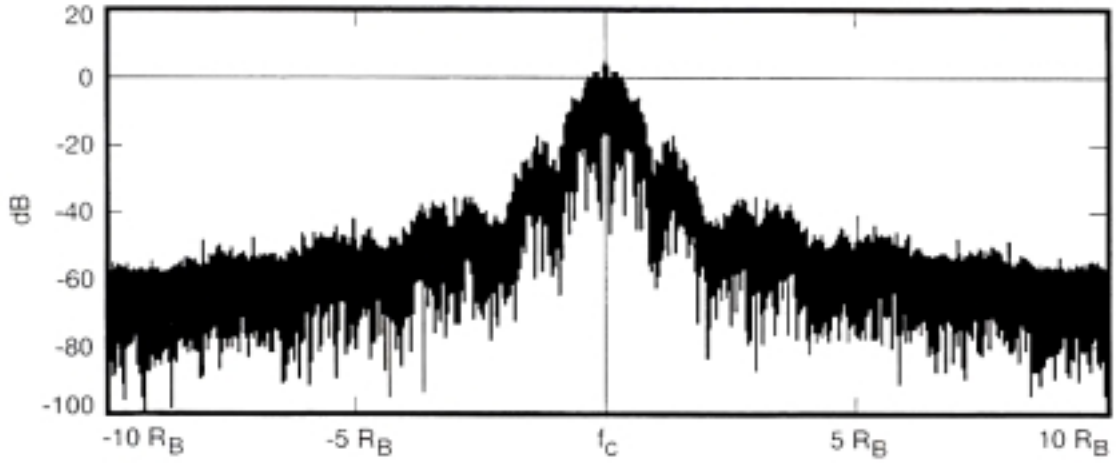

Figure 3-14b. Output of Power Amplifier

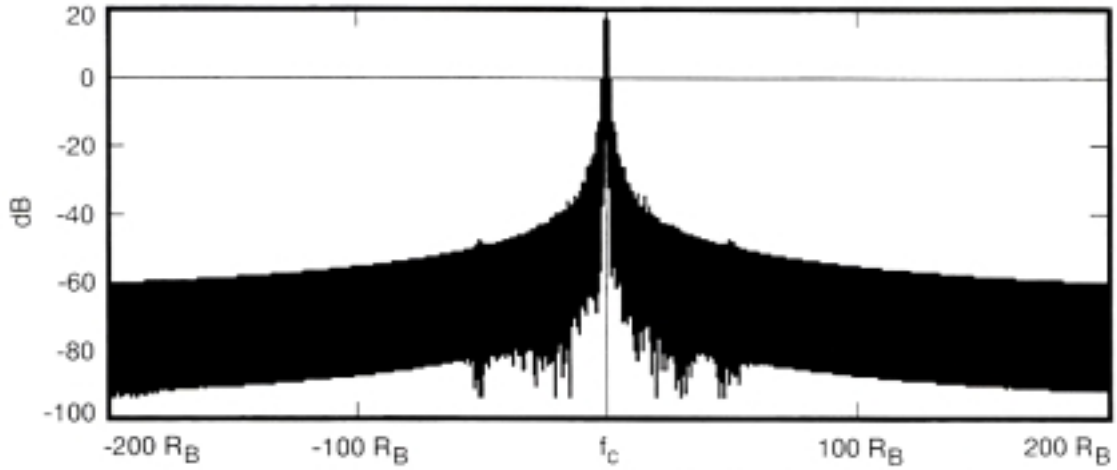

Figure 3-14c. Output of Second Harmonic Filter ($\pm$ 20 R_B)

Figure 3-14. Baseband Raised Cosine Filtered NRZ-L Data Spectra, α = 1 (Non-Ideal Data)

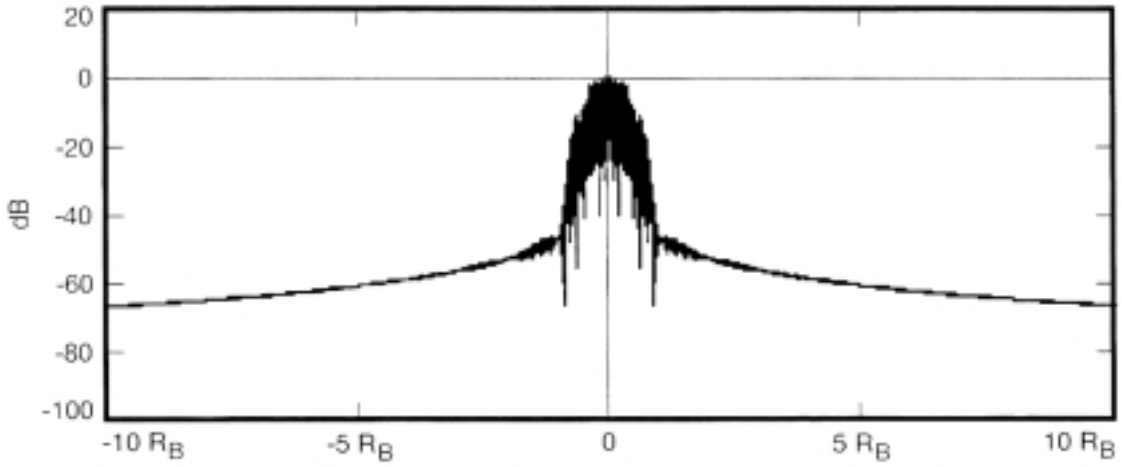

Figure 3-15a. Output from Square Root Raised Cosine Filter (α = 1; 2000 Taps)

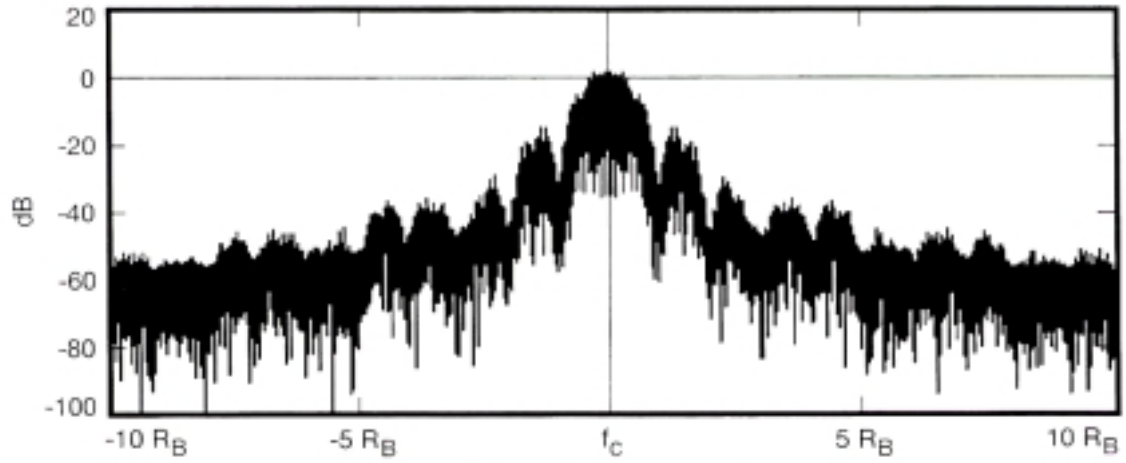

Figure 3-15b. Output of Power Amplifier

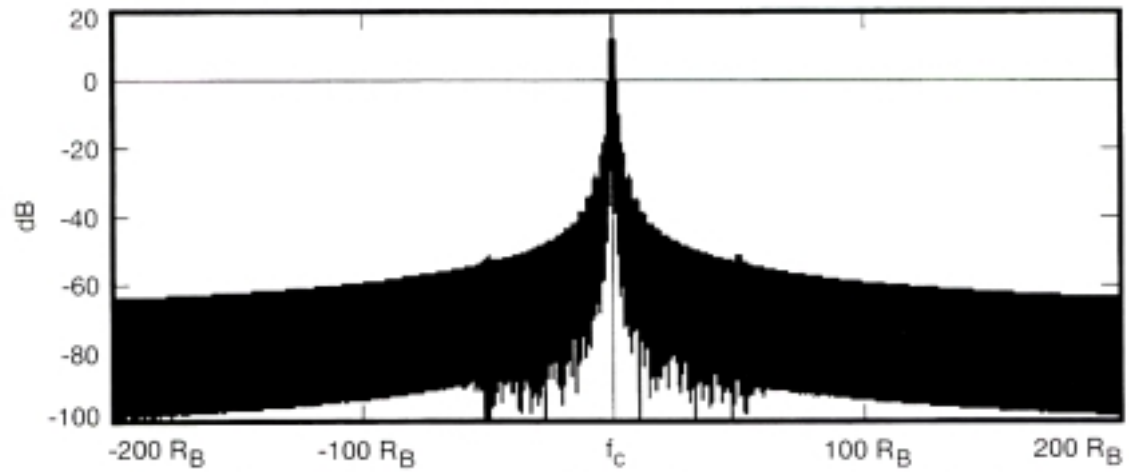

Figure 3-15c. Output of Second Harmonic Filter (± 20 R_B)

Figure 3-15. Baseband Square Root Raised Cosine Filtered NRZ-L Data Spectra, α = 1 (Ideal Data)

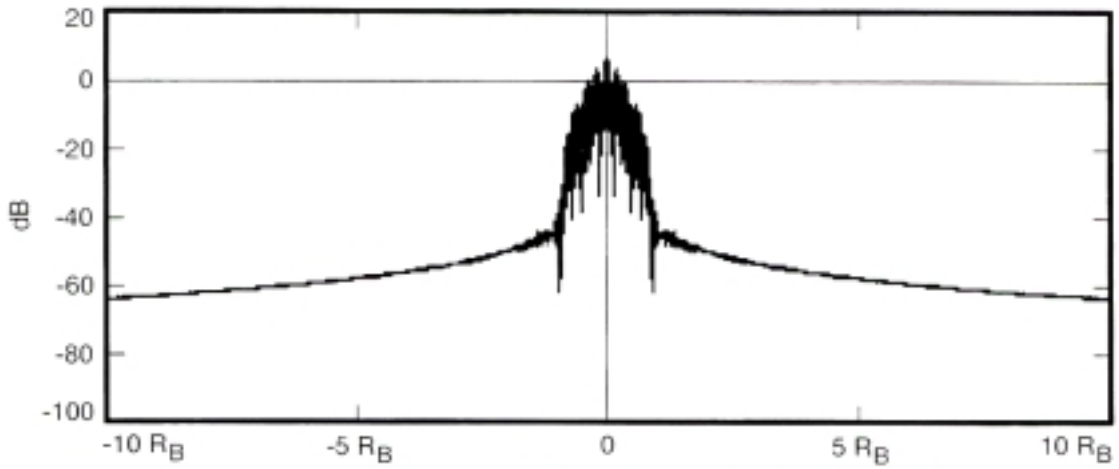

Figure 3-16a. Output from Square Root Raised Cosine Filter (α = 1; 2000 Taps)

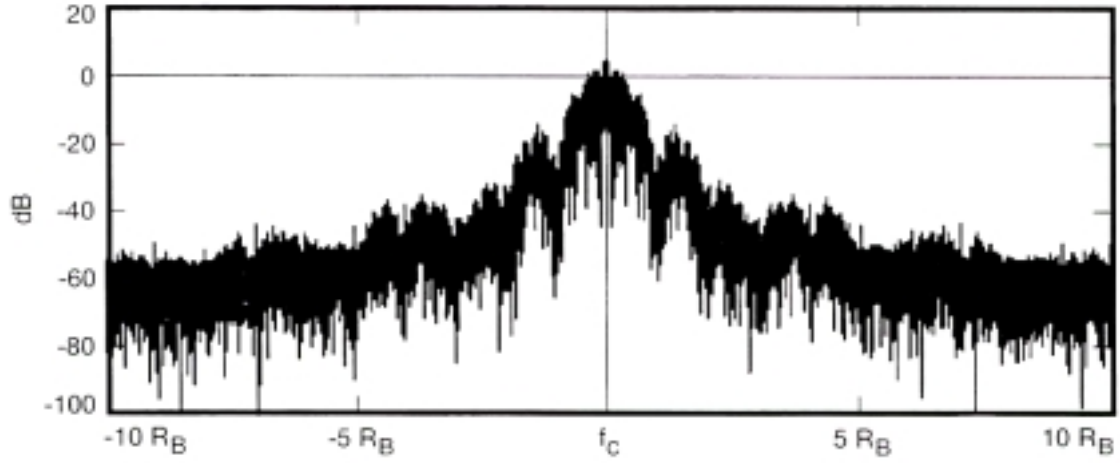

Figure 3-16b. Output of Power Amplifier

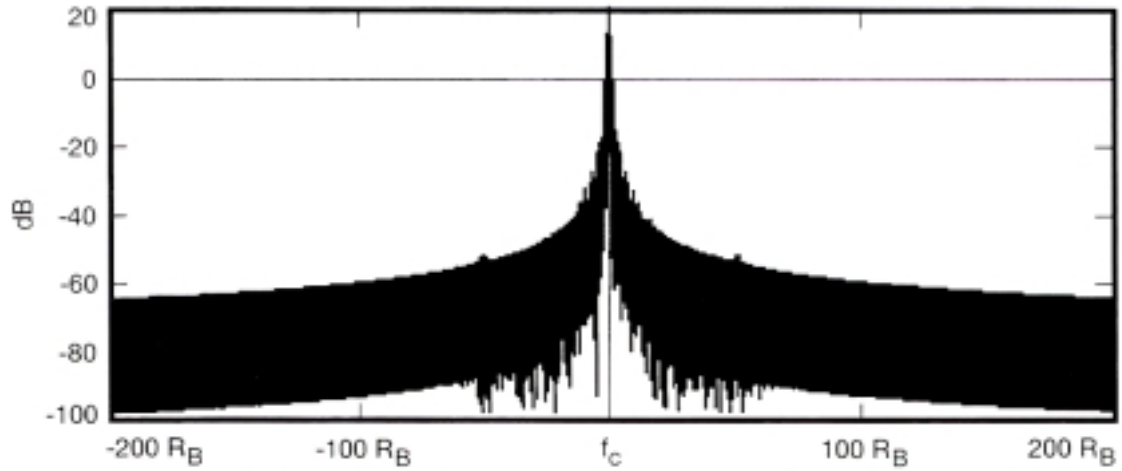

Figure 3-16c. Output of Second Harmonic Filter ($\pm$ 20 R_B)

Figure 3-16. Baseband Square Root Raised Cosine Filtered NRZ-L Data Spectra, α = 1 (Non-Ideal Data)

3.2.3.5 Raised Cosine Filter ($\alpha = 1$), Sampled Data

Since Raised Cosine filters only produce a true Raised Cosine function with Sampled data inputs as described in Section 3.2.3 above, simulations using Sampled data were made to determine whether the resulting spectra offered significant advantages over those produced by NRZ-L data. Figures 3-17a and 3-18a, for ideal and non-ideal data respectively, show the filter's output for Sampled data. The effects of sampling are evident from the small spikes seen in the Figures, particularly for the non-ideal data case.

These spikes are also clearly evident in Figures 3-17b and 3-18b representing the power amplifier's output. With a Sampled data input, the spectra for a Raised Cosine ($\alpha = 1$) filter begins to resemble those of the Butterworth and Bessel filters.

Following the second harmonic filter ($f_C \pm 20\ R_B$), Figures 3-17c and 3-18c, the spectrum appears to be similar to that for a Raised Cosine filter ($\alpha = 1$) with an NRZ-L input. However, measurements made with COMDISCO to determine the point where the frequency spectrum falls to a level 50 dB below the main data lobe show the performance with Sampled data is poorer than with NRZ-L data (see Tables 3-1a and 3-1b). This degraded performance results from the spikes generated by the data sampling process.

While it may be possible to reduce the amplitude or eliminate these emissions by a post filter signal processor, there is no evidence that the resulting spectrum would be better than a Raised Cosine filter with an NRZ-L input. However, amplitude studies discussed in Section 4 show that a Raised Cosine filter, with a Sampled data input, has a significantly more uniform output than one with an NRZ-L data input. Therefore, despite their poorer sideband attenuation, Raised Cosine filters with Sampled inputs may be useful in an operational system.

3.2.3.6 Square Root Raised Cosine Filter ($\alpha = 1$), Sampled Data

Figures 3-19a and 3-20a show the output of a Square Root Raised Cosine filter ($\alpha = 1$) with Sampled ideal and non-ideal data inputs respectively. Here the sampling effect is very evident and can be seen as a series of amplitude changes at intervals of approximately $0.1\ R_B$. These additional low level "spurious emissions" are likely the result of the Square Root Raised Cosine filter's wider bandwidth.

The power amplifier's output is shown in Figures 3-19b and 3-20b. Both exhibit significant levels of in-band spurious emissions with the result that they perform much like systems with Butterworth and Bessel filters.

Spurious emissions are clearly evident in the broadband spectrum ($f_C \pm 200\ R_B$) measured at the output of the second harmonic filter (Figures 3-19c and 3-20c).

The effect of these emissions is obvious in Tables 3-1a and 3-1b, for ideal and non-ideal data respectively, where the data sideband attenuation at $\pm$ 5 R_B is 14-16 dB less using a Sampled data input than is the case for an NRZ-L data input. Given the amplitude variations found for a Square Root Raised Cosine filter using a Sampled data input (see Section 4), it is questionable whether or not this filter with a Sampled data input will be useful.

3.3 Summary or Baseband Filter Simulations

Four filter types, seven different baseband filters, and four types of input data were studied to determine their effect in limiting the transmitted telemetry data spectrum's width. Most space agency's data systems produce an NRZ-L baseband format so it was selected as the primary input to the filters. However, because of their design, both the Raised Cosine and Square Root Raised Cosine filters were also evaluated using Sampled data inputs. To obtain the most realistic results, all simulations were performed with a non-ideal modulator, frequency multiplier, and solid-state power amplifier. For completeness, filters were tested using both ideal and non-ideal data as defined in Section 2.2.

A summary of the sideband levels for no baseband filtering and for the several baseband filter types appears in Tables 3-1a and 3-1b for ideal and non-ideal data respectively. Numbers in these Tables represent the highest signal levels, relative to the first (main) data lobe, found at the named (or greater) frequency on either side of the RF carrier. The attenuation provided by each filter can be found by subtracting the value in the first row, representing the unfiltered case, from the value for the desired filter at the same frequency. Numbers in these Tables were obtained from the COMDISCO simulator by positioning a cursor on the frequency spectrum at each of the specified frequency offsets and reading the amplitude directly from a digital representation on the screen. Accuracy of the measurement is believed to be within $\pm$ 2 dB.

Having completed the performance survey of the several filter types, the task becomes one of building a flight system. The most effective filter in the world, which produces the most compact RF spectrum, will be useless if flight and ground systems using the filter cannot be easily implemented. The characteristics of the several filters, as they relate to actual systems, are the subject of the next Section.

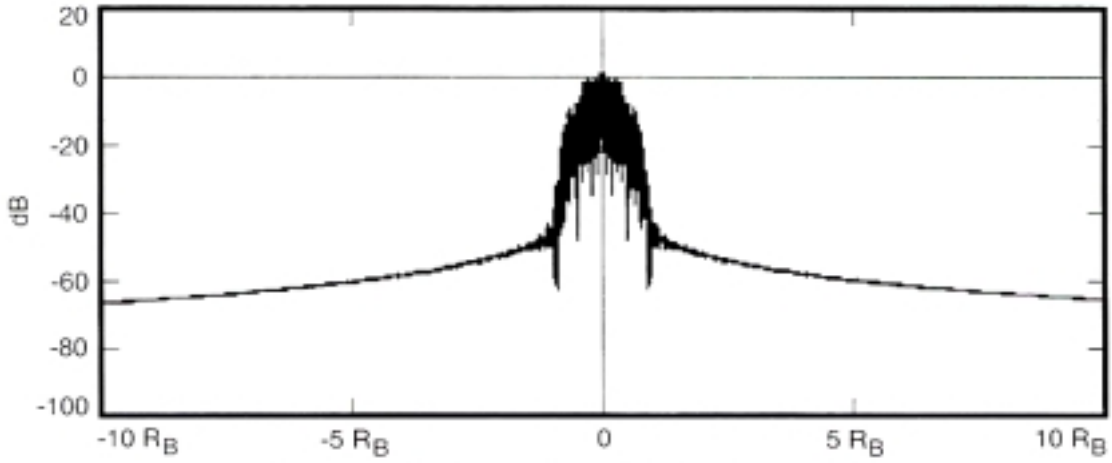

Figure 3-17a. Output from Raised Cosine Filter, $\alpha = 1$

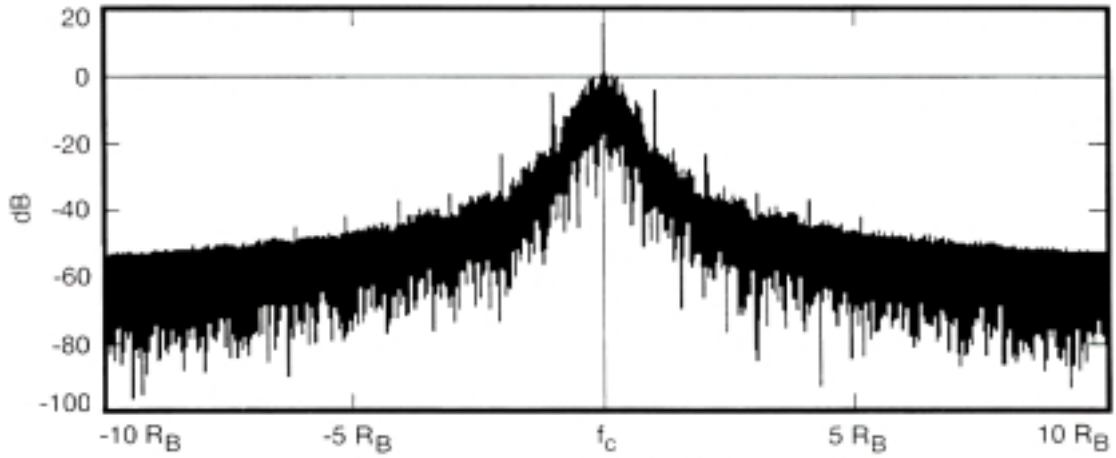

Figure 3-17b. Output of Power Amplifier

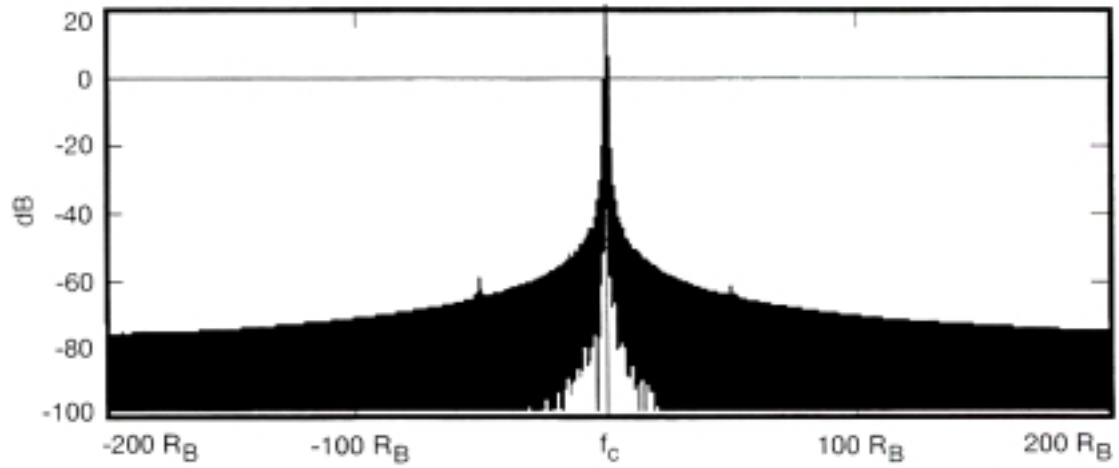

Figure 3-17c. Output of Second Harmonic Filter ($\pm$ 20 R_B)

Figure 3-17. Baseband Raised Cosine Filtered Sampled Data Spectra, $\alpha = 1$ (Ideal Data)

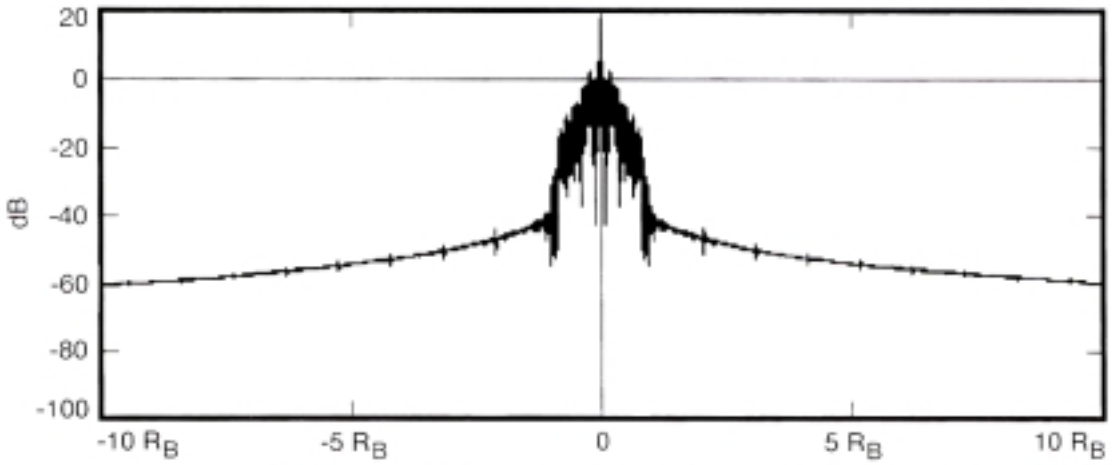

Figure 3-18a. Output from Raised Cosine Filter, $\alpha = 1$

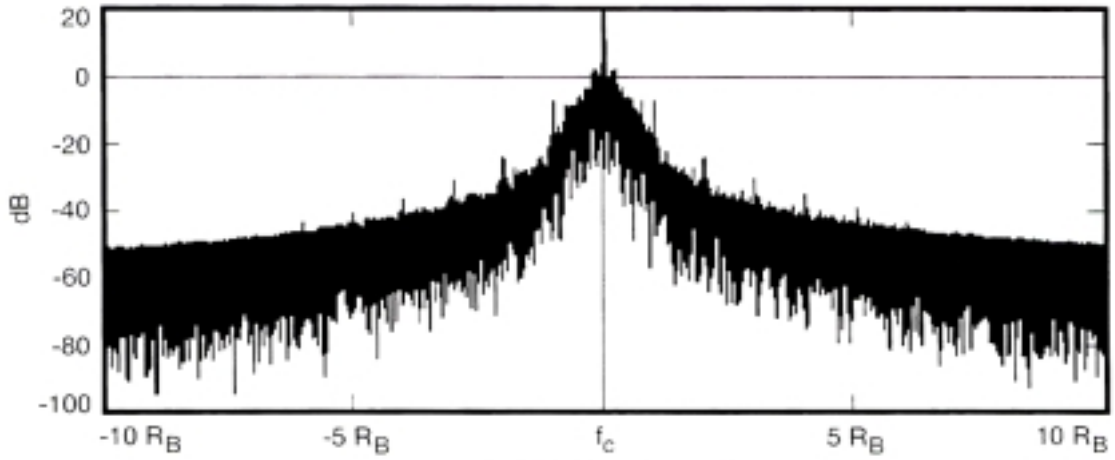

Figure 3-18b. Output of Power Amplifier

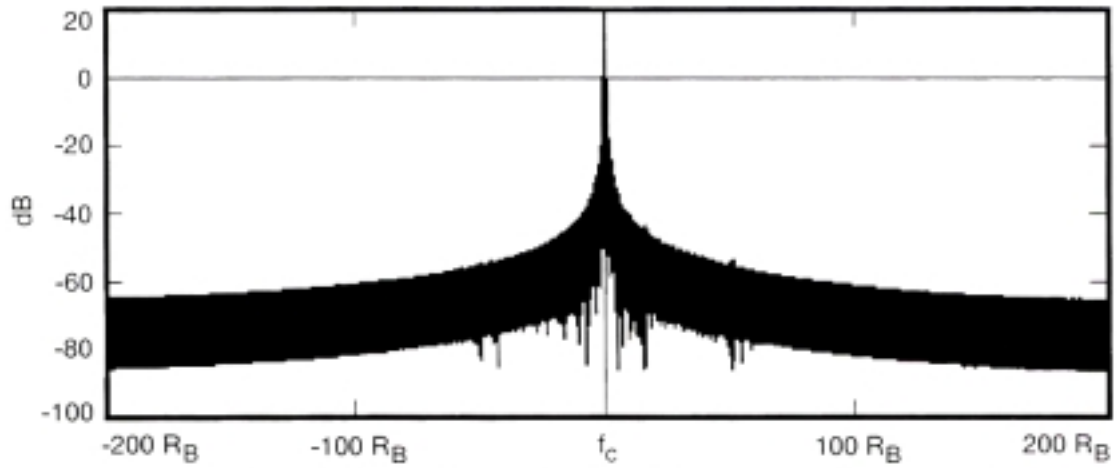

Figure 3-18c. Output of Second Harmonic Filter ($\pm$ 20 R_B)

Figure 3-18. Baseband Raised Cosine Filtered Sampled Data Spectra, $\alpha = 1$ (Non-Ideal Data)

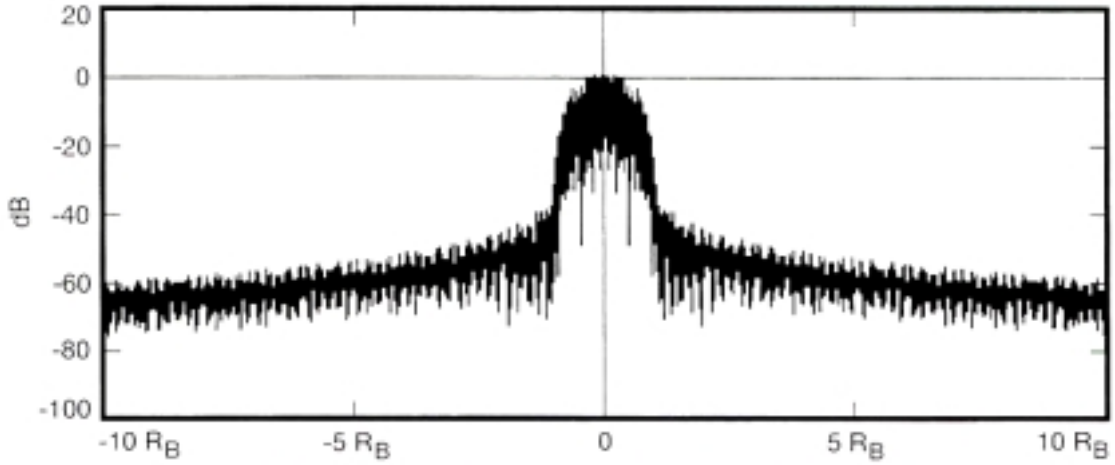

Figure 3-19a. Output from Square Root Raised Cosine Filter, $\alpha = 1$

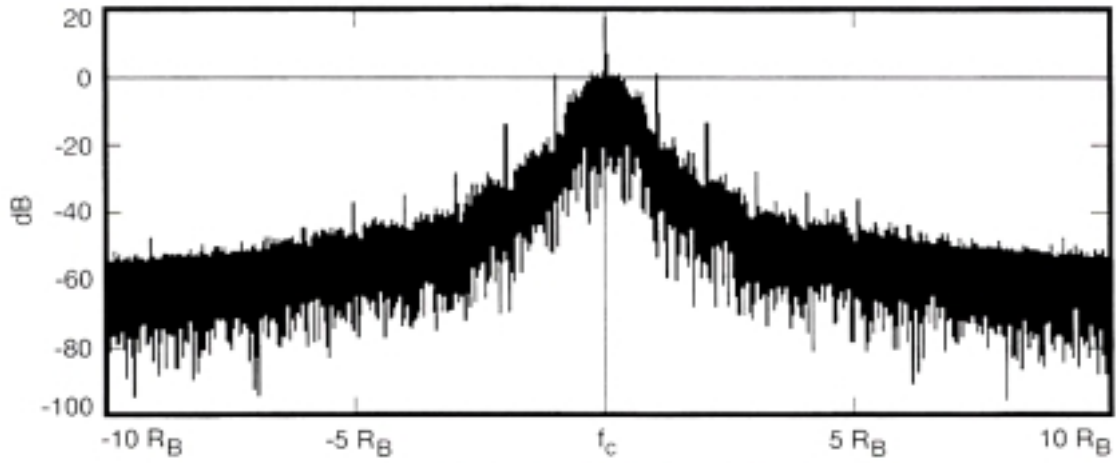

Figure 3-19b. Output of Power Amplifier

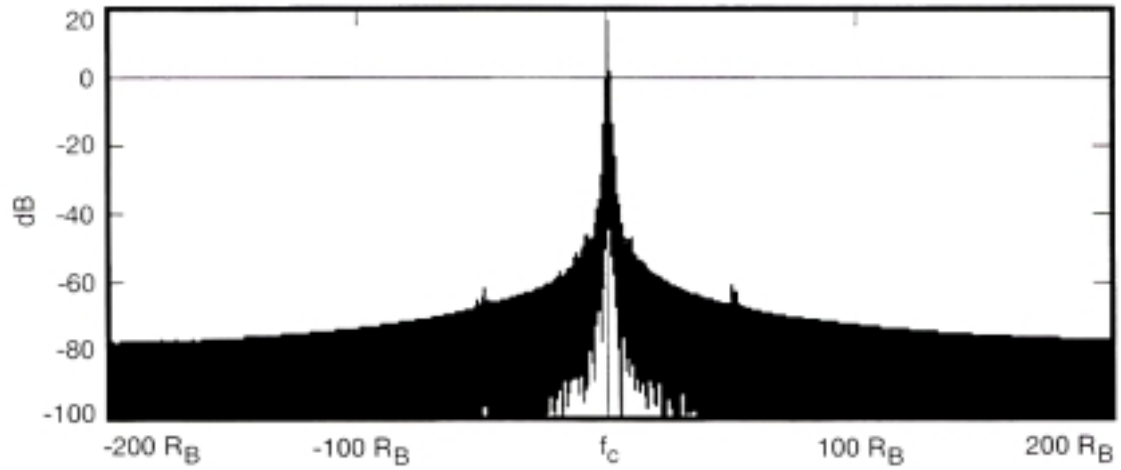

Figure 3-19c. Output of Second Harmonic Filter ($\pm$ 20 R_B)

Figure 3-19. Baseband Square Root Raised Cosine Filtered Sampled Data Spectra, $\alpha = 1$ (Ideal Data)

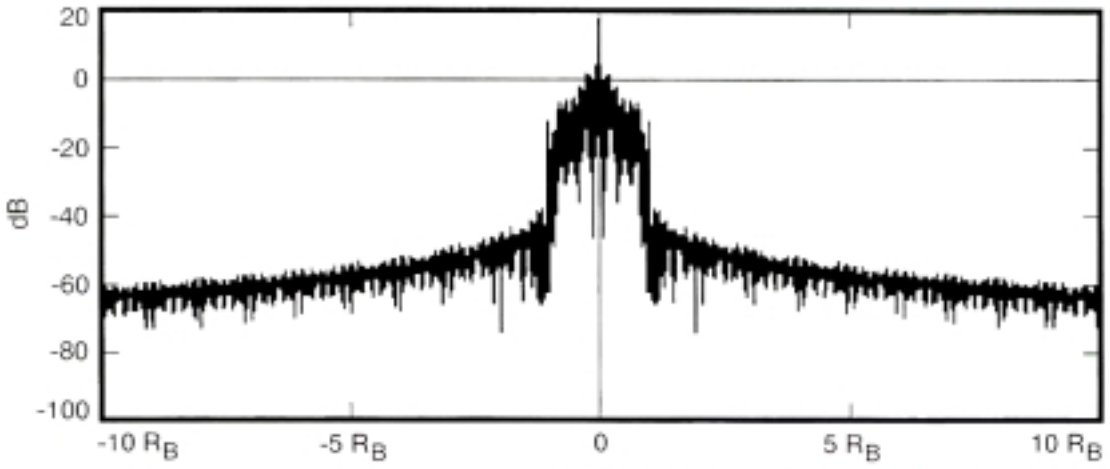

Figure 3-20a. Output from Square Root Raised Cosine Filter, $\alpha = 1$

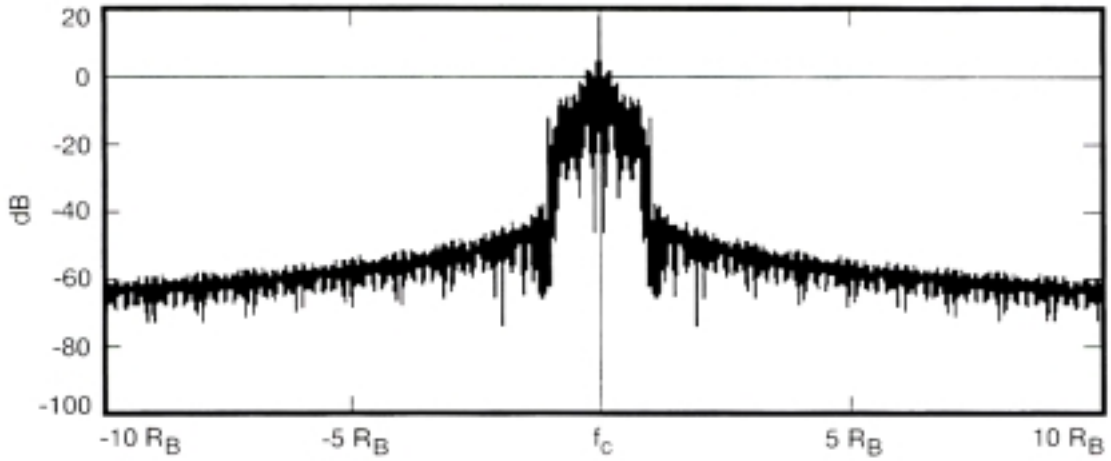

Figure 3-20b. Output of Power Amplifier

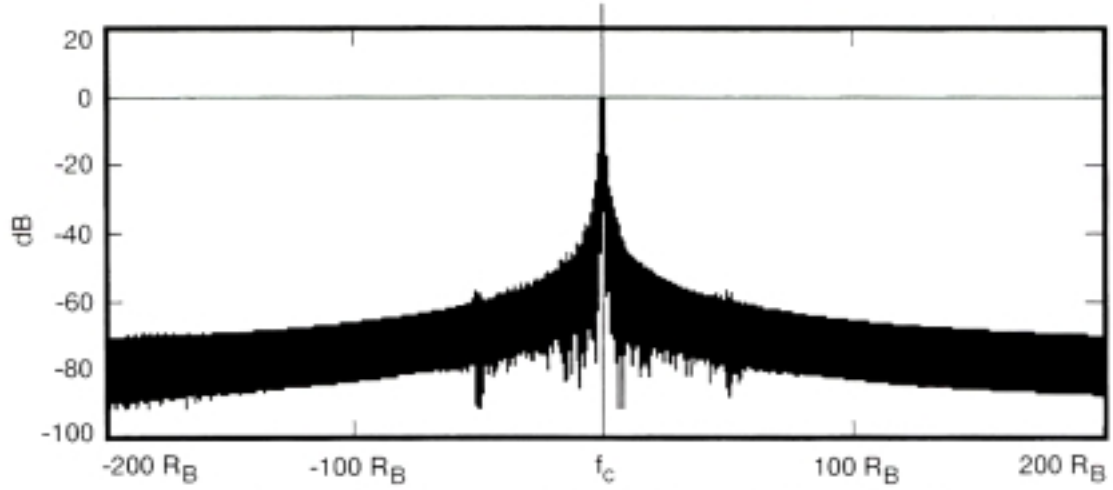

Figure 3-20c. Output of Second Harmonic Filter ($\pm$ 20 R_B)

Figure 3-20. Baseband Square Root Raised Cosine Filtered Sampled Data Spectra, $\alpha = 1$ (Non-Ideal Data)

Table 3-1a. Spectrum Levels Relative to First Data Sideband (Ideal Data)

Filter Type	± 0 R_B dB	± 5 R_B dB	± 10 R_B dB	± 20 R_B dB
None, Unfiltered Data (Reference)	0	-35	-39	-39
Butterworth, 5th Order	0	-45	-62	-65
Bessel, 3rd Order	0	-47	-58	-62
Raised Cosine (α = 0.25), NRZ-L Data	0	-54	-58	-64
Raised Cosine (α = 0.5), NRZ-L Data	0	-52	-59	-67
Raised Cosine (α = 1), NRZ-L Data	0	-52	-61	-66
Square Root Raised Cosine (α = 1), NRZ-L Data	0	-55	-59	-68
Raised Cosine (α = 1), Sampled Data	0	-49	-57	-63
Square Root Raised Cosine (α = 1), Sampled Data	0	-39	-54	-62

Table 3-1b. . Spectrum Levels Relative to First Data Sideband (Non-Ideal Data)

Filter Type	± 0 R_B dB	± 5 R_B dB	± 10 R_B dB	± 20 R_B dB
None, Unfiltered Data (Reference)	0	-25	-26	-29
Butterworth, 5th Order	0	-47	-61	-69
Bessel, 3rd Order	0	-45	-54	-62
Raised Cosine (α = 0.25), NRZ-L Data	0	-53	-59	-68
Raised Cosine (α = 0.5), NRZ-L Data	0	-52	-62	-69
Raised Cosine (α = 1), NRZ-L Data	0	-51	-63	-70
Square Root Raised Cosine (α = 1), NRZ-L Data	0	-53	-66	-71
Raised Cosine (α = 1), Sampled Data	0	-43	-54	-60
Square Root Raised Cosine (α = 1), Sampled Data	0	-39	-52	-59

4.0 SYSTEM CONSIDERATIONS

From Section 3 and Table 3-1b for non-ideal data, Raised Cosine and Square Root Raised Cosine filters appear to have a distinct advantage over the other types. Not only do they exhibit a smooth roll-off characteristic and have no discernable in-band spurious emissions, but also, the data sideband attenuation is greater than for Butterworth or Bessel baseband filters. Thus, the issue is one of determining whether these filter types are suitable for integration into space agencies' space-to-earth communications systems. This Section examines the practical application of the filters.

Two areas must be investigated to ascertain if these filters are useful in space telemetry systems. First, the filter's amplitude response to a random data pattern must be studied to determine its uniformity. Second, the Inter-Symbol Interference (ISI) must be measured to ensure that the losses are not excessive. Only if a filter provides acceptable performance in both of these areas should it be considered for a real communications system.

4.1 Filter Amplitude Response

Space agencies commonly employ phase modulation on their space-to-earth RF links. To minimize spacecraft telecommunications system redesign, each of the filters considered in Section 3 must be evaluated to determine whether or not it operates properly with existing spacecraft phase modulators. Between certain limits, a typical phase modulator in a residual carrier system will have a linear input voltage-to-output phase relationship. Thus, a linear change in input voltage will produce a linear change in RF phase at the output of the modulator. Generally, the linear region lies between approximately 0.1 to 1.4 radians of output phase shift.

Suppressed carrier modulators may be different. If the modulator's output phase is a nearly linear function of input voltage then the suppressed carrier and residual carrier systems will operate similarly. However, if the suppressed carrier modulator is switched (e.g., the output phase has only two [BPSK] or four [QPSK] discrete states which are largely independent of input voltage) then baseband filtering will not work because the output phase switches in 90 or 180 degree steps.

All filters studied in Section 3 were fed the same random NRZ-L or Sampled data. This test consisted of a 50-bit random NRZ-L data pattern, having differing run lengths of 1s and 0s, which was applied to each filter's input. Note that sometimes transitions occur at every bit-time.

[Bit Pattern = 11111111110000000000101010101000100001001011111011]

Here, the objective was to measure each filter's amplitude response to this bit pattern in order to judge whether or not a particular filter type produced an output that was suitable for a spacecraft communications system. The output amplitude for each filter type,

resulting from the random bit pattern, was plotted and variations in that amplitude were measured using COMDISCO in much the same way that the attenuation provided by each baseband filter was measured (see Section 3.3).

Each filter is considered in order and plots of its output amplitude appear in Figure 4-1. Amplitude variations were measured and are listed in Table 4-1 and represent the difference between the maximum and minimum values obtained at each filter's output from the random data pattern. Variations (% and dB) are referenced to the steady state value and show the amount of data sideband power deviation resulting from changes in data transition density. The large power variations found in the right-most column of Table 4-1 are because low transition density data approximates a squarewave while high transition density data is virtually a sinewave.

The random data pattern applied to all filters appears in Figure 4-1a and serves as a reference for subsequent filter evaluations. Ideally, a filter affects only the waveform and not the amplitude. Changes in amplitude are translated linearly into variations in phase angle by the modulator. Therefore, non-uniformity in input amplitude is translated into a change in data sideband power.

4.1.1 5th Order Butterworth Filter Response

Figure 4-1b shows the amplitude response of a 5th Order Butterworth filter to the random data pattern of Figure 4-1a. The filter's output is characterized by an overshoot at transitions which is probably the result of the filter's high Order (5th). Adjustment of the BT product may correct this overshoot. Variations between steady state (minimum) and peak (maximum overshoot) values can be as much a 26%.

Because of the complex waveform, it is difficult to compute the precise sideband power change as a function of transition density. However, an estimate of this power variation can be obtained by assuming that a long run of 1s or 0s (2 or more 1s or 0s) produces a squarewave modulating signal while transitions at every bit-time, passing through a filter with a BT product of 1.0, result in a waveform approximating a sine wave.

Using the CCSDS Link Design Control Table (DCT), the data sideband power was computed and noted for a squarewave modulating signal assuming that the peak of the squarewave data waveform corresponds to a modulation index of 1.2 radians. Thereafter, the DCT was reset for sinewave modulation and a new modulation index, corresponding to the peak of the overshoot (e.g., 1.26 x 1.2 radians = 1.51 radians), was entered. The new data sideband power was calculated and recorded. The power change between high and low transition density data was obtained by differencing the two computed sideband powers. **Note: this method is intended as an approximation of the total difference between steady state high and low transition density data and is not purported to be a precise measure.**

For the Butterworth filter, a power reduction of 1.4 dB for high transition density data was computed. Even with the overshoot at transitions, the high transition density data produced a somewhat lower transmitted sideband power because of its sinusoidal shape.

4.1.2 3rd Order Bessel Filter Response

Figure 4.1c depicts the output from a 3rd Order Bessel filter to the random data pattern. Here, the output is far more uniform than that of the 5th Order Butterworth filter. Measurements made using COMDISCO show that the variation is only 1.0%. Using the same technique described above, and assuming a 1.2 radian modulation index for the squarewave peak, the power decrease for high transition density data is 2.5 dB.

4.1.3 Raised Cosine Filter Response ($\alpha = 1$), NRZ-L Data

Full Raised Cosine ($\alpha = 1$) filters did poorly in this test (Figure 4d). Although the filter produced excellent waveforms, when the run-length of 1s or 0s exceeded 2, the amplitude variations for input data having transitions every bit-time are significant. COMDISCO measurements show the peak amplitude of high transition density data to be only 62% of the steady state amplitude. Using the same measurement method described above, and assigning a modulation index of 1.2 radians to the squarewave peak, the transmitted data sideband power is found to drop by 5.6 dB for high transition density data.

Amplitude variations cause two problems. First, the received E_B/N_O will be a function of data transition density. A significantly larger telemetry margin will be required for such systems to ensure that the Bit-Error-Rate (BER) does not increase to intolerable levels when long runs of alternating 1s and 0s occur.

Second, amplitude variations probably render Raised Cosine filters, with an NRZ-L input, useless in suppressed carrier systems. Assuming that the suppressed carrier system's modulator is linear and not switched (see Section 4.1), then it can be set to produce a uniform $\pm$ 90 degree peak modulation index for long runs (2 or more) of 1s or 0s.

However, when data transitions occur at each bit-time, the reduced amplitude at the filter's output results in a smaller modulation angle. Changing modulation angles, caused by varying data transition densities, produce a continually shifting reference phase in the receiver's Costas Loop. The result is a misalignment between the received signal's phase and the receiver's reference phase, which manifests itself as a data detection loss.

4.1.4 Square Root Raised Cosine Filter Response ($\alpha = 1$), NRZ-L Data

Figure 4.1e shows the amplitude response for a Square Root Raised Cosine ($\alpha = 1$) filter. The amplitude decline for high transition density data is far less prominent than that for a full Raised Cosine filter but it still falls to 86% of the steady state value. Using a modulation index of 1.2 radians for the squarewave peak value, the data sideband power decline for high transition density data is calculated to be 3.3 dB.

4.1.5 Raised Cosine Filter Response ($\alpha = 1$), Sampled Data

To complete the investigation of Raised Cosine filters, output amplitude changes were investigated using a Sampled data input. Figure 4-1f shows the filter's output response to a Sampled data pattern corresponding to the NRZ-L pattern in Figure 4-1a. Recall that for Sampled data, a pulse of short duration and an amplitude of + 1 represents a "1" while an equally short pulse with an amplitude of -1 represents a "0".

Comparing Figures 4-1f and 4-1d reveals that Sampled data greatly reduces the amplitude variation between high and low transition density data. Whereas an NRZ-L input causes amplitude changes of 38%, Sampled data reduces the difference to only 6% (see Table 4 1). Recall that the power variations in the right-most column of Table 4-1 are largely because low transition density data approximates a squarewave while high transition density data is virtually a sinewave having a lower RMS power than a squarewave.

In Section 4.1.3 it was concluded that the amplitude variation from a Raised Cosine filter using an NRZ- L input was too large to make this filter type suitable in most systems, particularly where suppressed carrier modulation is employed. Using a Sampled data input, most of the amplitude changes disappear which may make this type of filter useable in some applications. However, spectrum studies in Section 3, using non-ideal data, determined that the sideband attenuation for a Raised Cosine filter with a Sampled data input was 8 dB poorer at $\pm$ 5 R_B than was the case for a Raised Cosine Filter with an NRZ-L data input. In fact, its performance was 2 and 4 dB poorer than the Bessel and Butterworth filters respectively making its value doubtful (see Table 3-1b).

4.1.6 Square Root Raised Cosine Filter Response ($\alpha = 1$), Sampled Data

Figure 4-1g shows the amplitude response of a Square Root Raised Cosine ($\alpha = 1$) filter to Sampled data. At first, the filter seems unusable due to the large amplitude variations (22%) and the presence of the individual pulses comprising each bit. However, note that the high transition density data has a greater amplitude than does the low transition density data. Applying the power measurement technique used for the other filters and recalling that low transition density data is similar to a squarewave while high transition density data

approximates a sinewave, the data sideband power change was found to be only 1.3 dB.

Nevertheless, the issue is whether a Square Root Raised Cosine filter with a Sampled data input is useful in a real space communications system. Returning to Table 3-1b for non- ideal data, the sideband attenuation at $\pm$ 5 R_B is found to be 14 dB poorer when Sampled data, rather than NRZ-L data, is used. Both the Butterworth and Bessel filters perform substantially better in both sideband attenuation and uniformity of output than does a Square Root Raised Cosine (α = 1) filter using Sampled data.

4.1.7 Summary or Filter Output Amplitude Variation Study

Amplitude variation measurements are summarized in Table 4-1 for each of the filters. While the power changes appear to be excessive, the computational method is likely to represent a "worst case" and most of the variation is due the squarewave to sinewave conversion. No attempt was made to "optimize" any of the filters and doing so may improve the amplitude uniformity. Additionally, amplitude changes become irrelevant if the data transition density becomes constant as would be the case with Bi-ϕ modulation. Furthermore, convolutional encoding and/or data randomization will increase the data transition density although it cannot assure a uniform density. Further study is required to determine which filters, if any, are useful in suppressed carrier systems.

As discussed in Section 4.1.5, the amplitude changes found with Raised Cosine filters can be substantially eliminated by employing a sampling technique. Amplitude plots for such filters are very similar to that for a Bessel filter in which the peak amplitude is independent of transition density.

Table 4-1. Filter Amplitude Variation to Random Data Pattern

Filter Type	Maximum Value	Minimum Value	Variation %	Variation dB
5th Order Butterworth, NRZ-L	$\pm$ 1.26	$\pm$ 1.0	21	1.4
3rd Order Bessel, NRZ-L	$\pm$ 1.02	$\pm$ 1.01	1	2.5
Raised Cosine (α = 1), NRZ-L	$\pm$ 1.02	$\pm$ 0.63	38	5.6
Square Root Raised Cosine (α = 1), NRZ-L	$\pm$ 1.04	$\pm$ 0.90	13	3.3
Raised Cosine (α = 1), Sampled	$\pm$ 1.07	$\pm$ 1.0	6	2.8
Square Root Raised Cosine (α = 1), Sampled	$\pm$ 1.47	$\pm$ 1.15	22	1.3

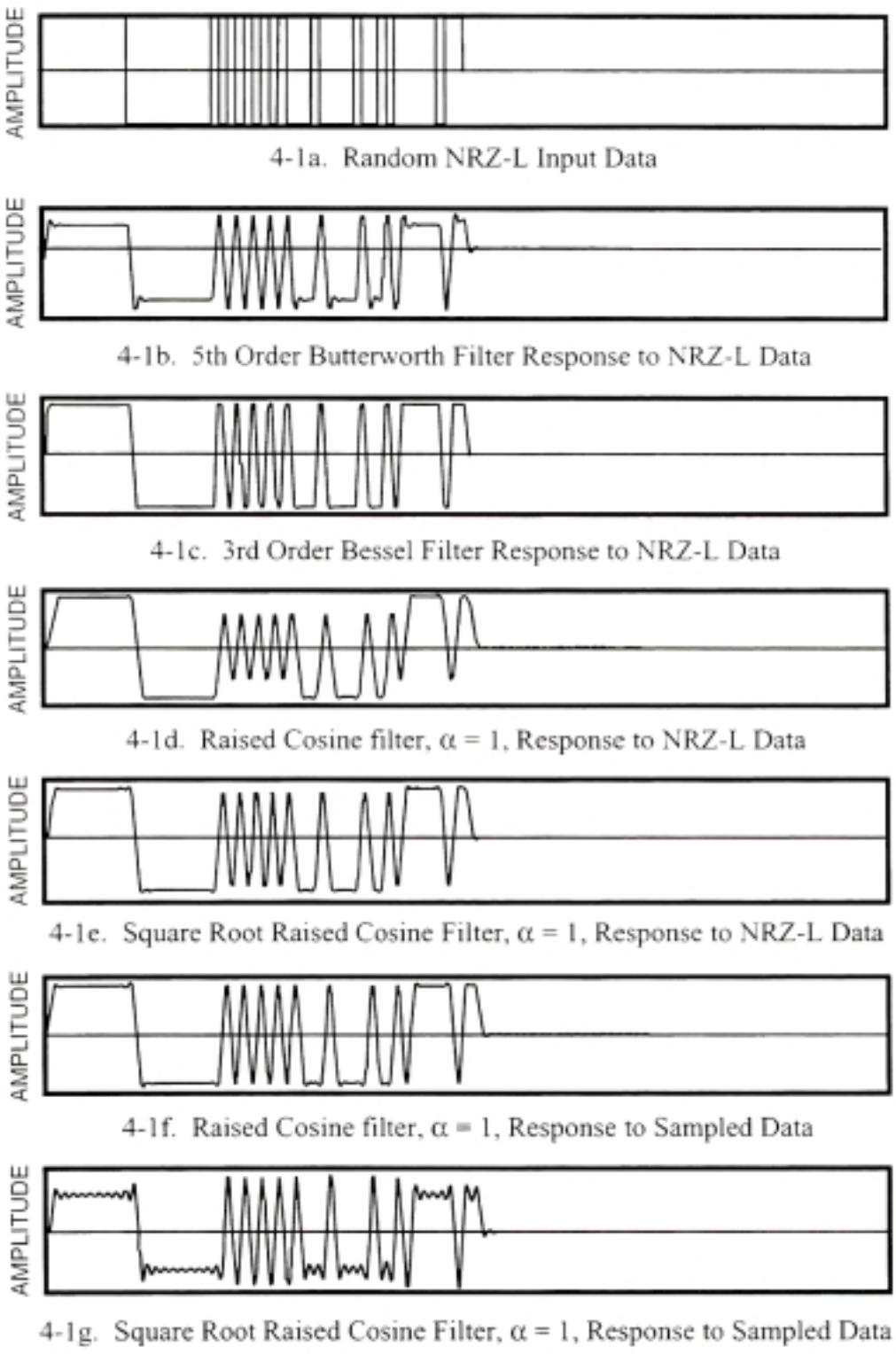

Figure 4-1. Filter Amplitude Responses to Random NRZ-L and Sampled Data

4.2 Inter-Symbol Interference (ISI)

A filter may be very effective in limiting the transmitted data spectrum and yet render the communications system useless if the Inter-Symbol Interference (ISI) is too high. As noted in Section 4.1, inserting a baseband data filter affects the transmitted data symbol's waveform. For ideal data, what was once a perfect pulse (e.g., zero rise and fall times and complete data symmetry) will begin to exhibit longer and longer data symbol rise and fall times as the baseband filter's bandwidth is narrowed. A well-designed filter should not introduce data asymmetry but the data symbol will begin to approximate a sinewave as the higher order harmonics are attenuated by the filter. **Eliminating the high order data harmonics is the principal reason that the bandwidth of the transmitted data spectrum is reduced as the filtering is increased.**

Some filters elongate the data symbol. When that happens, the trailing edge of one symbol begins to overlap the leading edge of the following symbol. The interference resulting from this Inter- Symbol Interference (ISI) produces a loss because the distinguishability of individual symbols has been reduced. Such loss must be accounted for in the Link Design Control Table (DCT) since it adversely affects the data channel's capacity. For example, ISI losses occurring in the telemetry system would be entered at line 75 of the CCSDS DCT.

Calculations of the ISI were made for each of the passive filters included in this study. As stated-above, both the Butterworth and Bessel filter's bandwidths were set at $\pm$ 1 R_B and the BT product was equal to 1.0 in order to compare the transmitted data spectra from these filters with those from the Raised Cosine and Square Root Raised Cosine filters. Such narrow filtering most certainly increases the ISI for those two filter types shown in Table 4-2 below. However, even with the narrow Butterworth and Bessel filter bandwidths, the transmitted data spectra obtained with Raised Cosine and Square Root Raised Cosine (α = 1) filters, using NRZ-L inputs, are materially better than the former types (see Table 4-1).

NOTE: The ISI losses reported in Table 4-2 for the Butterworth and Bessel cases are for two filters only, one at the transmit end and one matched filter at the receive end. Effects of the modulator, multiplier, power amplifier, and other system components have not been included. Since only the effects of the filters are being investigated, Ideal Data is used for this part of the study.

Determining the ISI for Raised Cosine and Square Root Raised Cosine filters requires an examination of the Eye Diagrams for each of the filters. An Eye diagram is constructed by overlaying a digital data stream, which has undergone filtering, on a single amplitude plot whose time scale covers interval: -T < t < T. An ISI-free sample point exists where all lines, representing the data symbols, cross one another simultaneously.

Theoretically, a pair of Raised Cosine filters (α = 1), operating in a linear communications system with one filter at the transmitting end and the other at the receiving end, will exhibit at least one ISI-free sample point. A pair of Square Root Raised Cosine filters, similarly located and operating under the same conditions, will exhibit at least two ISI-free sample points.

Figures 4-2 and 4-3 are eye diagrams for Raised Cosine and Square Root Raised Cosine (α = 1) filters using NRZ-L and Sampled data respectively. Two eye diagrams, generated with ideal data, are presented for each case. The first represents the output of the spacecraft's baseband filter while the second depicts the output of a second, identical filter after the signal has passed through the solid-state power amplifier. Since modulator and multiplier nonlinearities can be controlled, they were not included in these simulations.

4.2.1 Raised Cosine and Square Root Raised Cosine Filter Eye Diagrams, NRZ-L Data

Figure 4-2 contains eye diagrams for Raised Cosine and Square Root Raised Cosine filters using NRZ-L data inputs. Figure 4-2a shows the eye diagram at the data source for a Raised Cosine (α = 1) filter output over an interval of 2T. Note the existence of a single ISI-free sample point per symbol at 0.5T where all lines converge.

Figure 4-2b represents the output of the second Raised Cosine (α = 1) filter after the signal has passed through the nonlinear power amplifier. Here there are no ISI-free sample points. In fact, the comparative chaos of the diagram suggests that the nonlinearities may introduce a substantial amount of ISI. While it has not been possible to measure the ISI level at this writing, the diagram suggests that an alternative filtering and detection system at the receiving end should be investigated.

Similar results were found for the Square Root Raised Cosine (α = 1) filter using NRZ-L data. Figure 4-2c showing the baseband filter output on the data source side has two ISI-free sample points per symbol at 0.25T and 0.75T. Conversely, Figure 4-2d depicts the output of the second Square Root Raised Cosine (α = 1) filter after the signal has passed through the nonlinear power amplifier. Again, no ISI-free sample points exist. However, this diagram is less chaotic than Figure 4-2b suggesting that the ISI level may be lower for this filter combination than is the case for the two Raised Cosine filters.

4.2.2 Raised Cosine and Square Root Raised Cosine Filter Eye Diagrams, Sampled Data

Figure 4-3 contains eye diagrams for both Raised Cosine and Square Root Raised Cosine filters using Sampled data. As does Figure 4-2a, Figure 4-3a represents the spacecraft's Raised Cosine (α = 1) baseband filter output. It exhibits a single ISI-free sample point per symbol at 0.5T. Figure 4-3b depicting

the output of the second, identical Raised Cosine filter following the power amplifier has no ISI-free sample points. However, like the previous case, the comparative order of the diagram may suggest lower ISI levels than is the case with the same filter receiving NRZ-L data.

Figure 4-3c shows the output of a Square Root Raised Cosine ($\alpha = 1$) filter with a Sampled data source. Like Figure 4-2c, two ISI-free points per symbol are present at 0.25T and 0.75T. However, Figure 4-3d, depicting the second Square Root Raised Cosine ($\alpha = 1$) filter's output following power amplification, is more chaotic than that for the Raised Cosine filter. It is unclear, from an ISI point of view, whether Square Root Raised Cosine filters will fair better with NRZ-L or Sampled data inputs. Further study is necessary to make this determination as well as to compute the actual ISI levels.

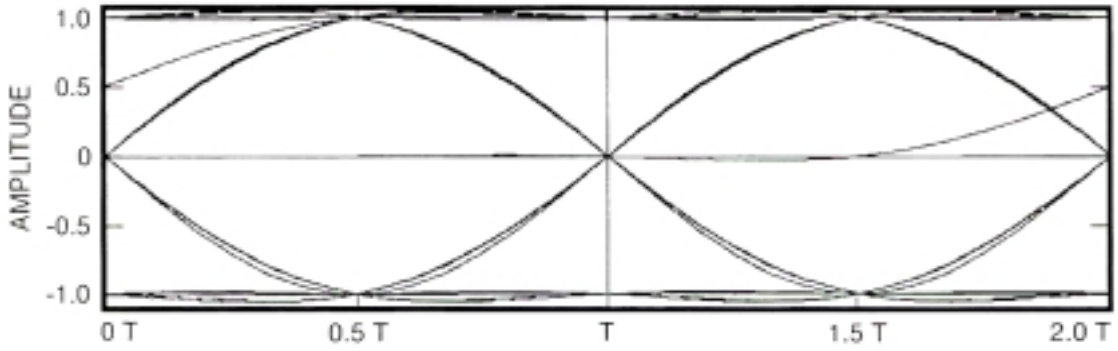

Figure 4-2a. Baseband Filter Output, Single Raised Cosine Filter (α = 1)

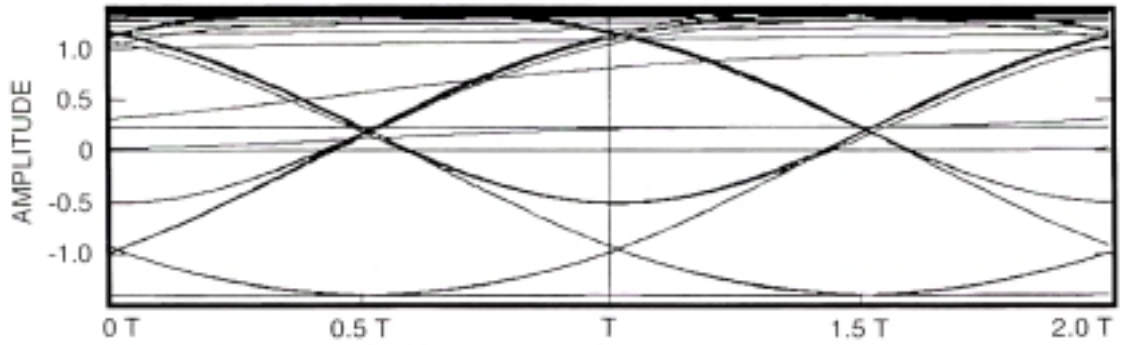

Figure 4-2b. Receiver Filter Output, Two Raised Cosine Filters (α = 1)

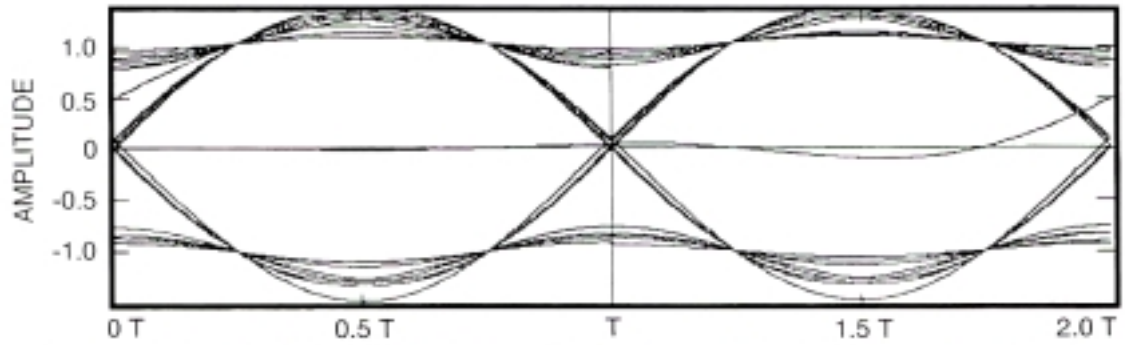

Figure 4-2c. Baseband Filter Output, Single Square Root Raised Cosine Filter (α = 1)

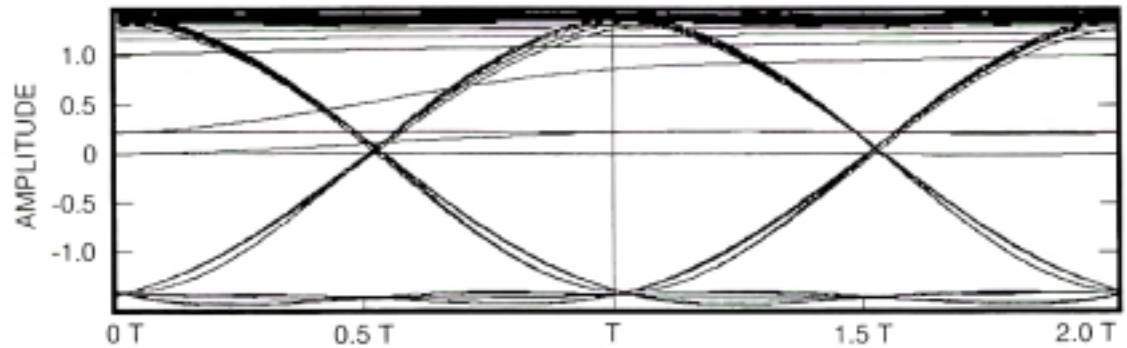

Figure 4-2d. Receiver Filter Output, Two Square Root Raised Cosine Filters (α = 1)

Figure 4-2. Eye Diagrams for Raised Cosine Filters (α = 1), Ideal NRZ-L Data in a Non-Linear Channel

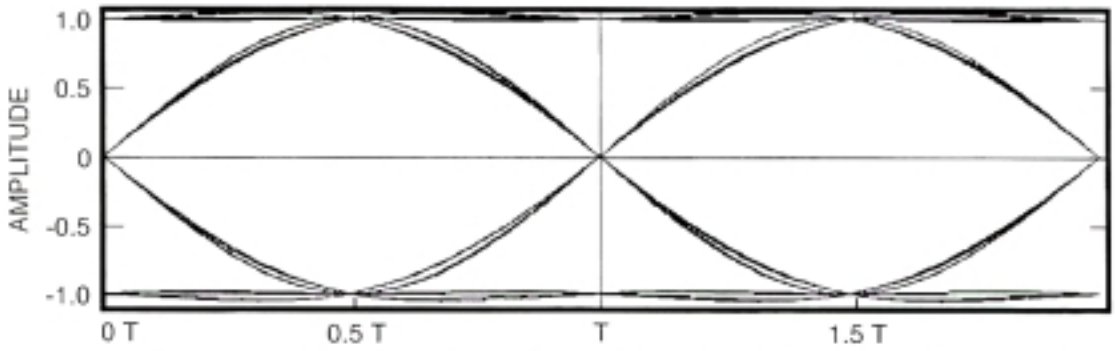

Figure 4-3a. Baseband Filter Output, Single Raised Cosine Filter ($\alpha = 1$)

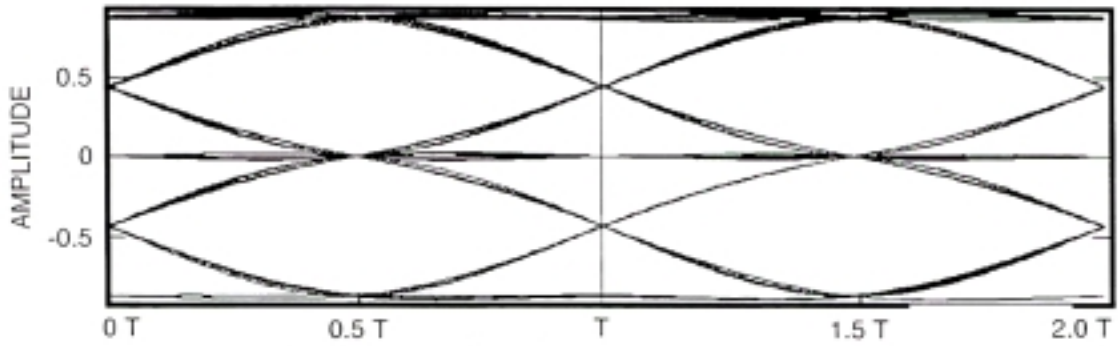

Figure 4-3b. Receiver Filter Output, Two Raised Cosine Filters ($\alpha = 1$)

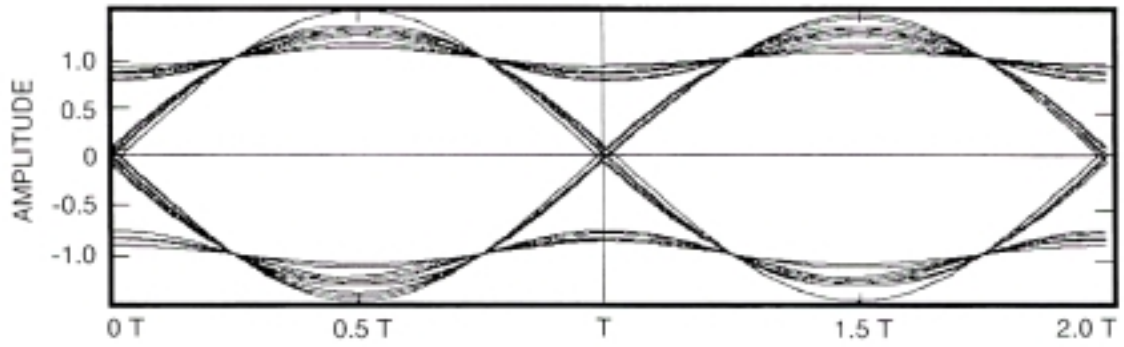

Figure 4-3c. Baseband Filter Output, Single Square Root Raised Cosine Filter ($\alpha = 1$)

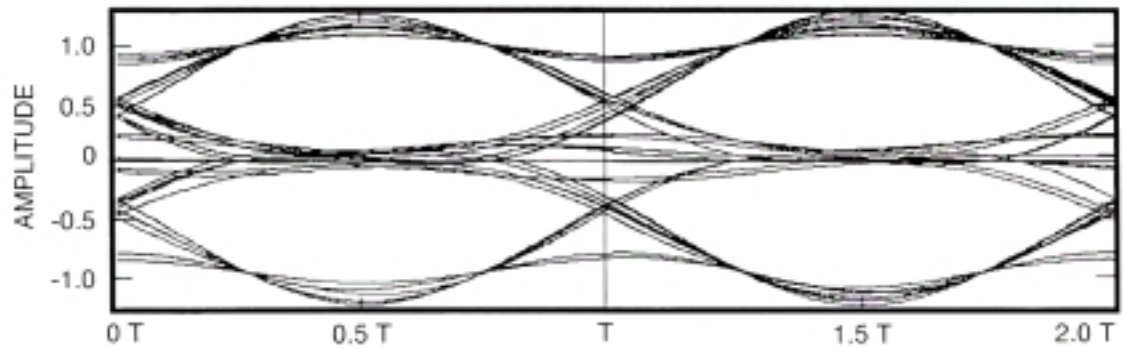

Figure 4-3d. Receiver Filter Output, Two Square Root Raised Cosine Filters ($\alpha = 1$)

Figure 4-3. Eye Diagrams for Raised Cosine Filters ($\alpha = 1$), Ideal Sampled Data in a Non-Linear Channel

4.2.3 Summary of ISI Studies

For passive filters such as the Butterworth and Bessel types, bandwidths greater than 1 R_B will be required to achieve reasonable ISI levels. While this will increase the transmitted frequency spectrum's width, their simplicity and comparatively good performance makes them candidates worth considering.

Raised Cosine and Square Root Raised Cosine filters pose more of a problem. The lack of any ISI-Free sample points, after the signal has passed through nonlinear system elements, makes their application questionable. However, the superior sideband attenuation of a Square Root Raised Cosine (α = 1) filter using NRZ-L data makes it a very attractive candidate.

Perhaps alternative filtering and sampling techniques can be found which will permit using Square Root Raised Cosine filters while obtaining reasonable ISI levels. Further studies in Phase 3 will be needed to determine whether or not a viable system design using Square Root Raised Cosine filters is feasible.

TABLE 4-2: INTER-SYMBOL INTERFERENCE FOR FILTER PAIRS (Ideal Data and Components)

BASEBAND FILTER TYPE	ISI @ $\pm$ 1 R_B dB	ISI @ $\pm$ 2 R_B dB	ISI @ $\pm$ 5 R_B dB
Unfiltered Baseband NRZ-L Data, Reference	0	0	0
Butterworth Baseband Filter, 5th Order, NRZ-L Data	-0.85	-0.47	-0.23
Bessel Baseband Filter, 3rd Order, NRZ-L Data	-1.51	-0.61	-0.24
Raised Cosine Baseband Filter (α = 1), NRZ-L Data	TBD	TBD	TBD
Square Root Raised Cosine Baseband Filter (α = 1), NRZ-L Data	TBD	TBD	TBD
Raised Cosine Baseband Filter (α = 1), Sampled Data	TBD	TBD	TBD
Square Root Raised Cosine Baseband Filter (α = 1), Sampled Data	TBD	TBD	TBD

NOTE:

TBD ISI values for Raised Cosine and Square Root Raised Cosine filters have not been computed at this time. Further investigation will be necessary in Phase 3 to determine their behavior in nonlinear channels and to design the optimum filtering and detection system.

5.0 PHASE 2 SUMMARY

This investigation of baseband filters and their effect on the transmitted telemetry data's spectrum shows that such filters can significantly narrow the transmitted RF bandwidth. Data sideband power reductions from 22 - 28 dB at $\pm$ 5 R_B and 29 - 41 dB at $\pm$ 10 R_B appear to be feasible using the filters described in this paper. These reductions were obtained with non-ideal data and hardware and with no effort devoted to filter optimization. With some effort, greater attenuations may be obtainable.

At this juncture, the real issues are:

1. *Can the number of spacecraft using a specific frequency band be increased if baseband filtering is employed?*

2. *If the number of spacecraft using a specific frequency band can be increased, how many more can be accommodated than would be the case if no filtering is used?*

To estimate the value of baseband filtering, one can compare the number of missions with filtering which will fit into a frequency allocation to the number fitting into the same allocation but which do not have such filtering. This frequency band *Utilization Ratio* (ρ) is found from the relationship:

$$\rho = \frac{\text{Number of Spacecraft with Filtering Accommodated in Frequency Band}}{\text{Number of Spacecraft without Filtering Accommodated in Frequency Band}}$$

Finding this ratio requires making certain assumptions. Foremost among these is the acceptable interference level from spacecraft operating on adjacent channels. Such a calculation is complicated by the fact that each spacecraft has a unique data rate and power spectral density, which affects the frequency separation required to avoid interference. Additional frequency separation will be needed because of each spacecraft's Doppler frequency shifts.

However, guard-bands to provide RF isolation between several missions exhibiting differing characteristics will be required irrespective of whether or not baseband filtering is utilized. H the allocated frequency band is sufficiently large to accommodate many spacecraft, and the guard bands are assumed to be small compared to the missions' assigned [noticed] bandwidths, then the existence of these guard bands will not have a large effect on the *Utilization Ratio*.

An estimate of the increased spectrum utilization can be obtained by making a few additional simplifying assumptions:

1. All spacecraft have the same data rate with identical EIRPs and PFDs.

2. Spectra from spacecraft in adjacent channels will be permitted to overlap one another provided that, at the frequency where the overlap occurs, the signals are at least 50 dB below that of the main telemetry lobe (1st data sideband).

Here, the 50 dB is an arbitrary value and the reader can substitute any other desired number. Like the frequency guard band between adjacent spacecraft, the level selected where spectral overlap is permitted will not make a first order change in the *Utilization Ratio*. Only the total number of spacecraft, which can be placed in the allocated frequency band, will vary.

COMDISCO measurements were made using unfiltered ideal and non-ideal data, with the second harmonic filter removed, to determine the frequency at which the data spectrum was 50 dB below the main lobe. Spectra for each of the filter types in Section 3 was used to determine the frequency at which total data power fell to 50 dB below the main data lobe. Using the two numbers, the *Utilization Ratio* was computed using the relationship above. Table 5-1 summarizes the results.

TABLE 5-1. SUMMARY OF UTILIZATION RATIO IMPROVEMENT

Filter Type	Ideal Data -50 dB Pt.	Ideal Data Util. Ratio (ρ)	Non-Ideal Data -50 dB Pt.	Non-Ideal Data Util. Ratio (ρ)
Unfiltered, Reference	35 R_B	-	51 R_B	-
Butterworth, 5th Order	6 R_B	5.8	5.7 R_B	8.9
Bessel, 3rd Order	6 R_B	5.8	6 R_B	8.5
Raised Cosine (α = 1), NRZ-L	4.9 R_B	7.1	4.9 R_B	10.4
Sq Rt Raised Cosine (α = 1), NRZ-L	4.6 R_B	7.6	4.7 R_B	10.8
Filter Averages, NRZ-L Data:	**5.4 R_B**	**6.6**	**5.3 R_B**	**9.6**
Raised Cosine (α = 1), Sampled Data	5.6 R_B	6.2	6 R_B	8.5
Sq Rt Raised Cosine (α = 1), Samp. Data	6.8 R_B	5.1	6.3 R_B	8.1
Filter Averages, Sampled Data:	**6.2 R_B**	**5.6**	**6.2 R_B**	**8.3**

From the averages, is clear that baseband filtering offers a significant potential for increasing the number of spacecraft operating in a given frequency band, particularly if there is data asymmetry. Bandwidth utilization can potentially increase from 6 to 10 times, compared to unfiltered data, depending upon the data's condition, baseband filter type, and data type (NRZ-L or Sampled).

The importance of this finding is best illustrated with an example. H baseband filtering is applied in the present 90 MHz wide Category A 2 GHz band, the potential increased utilization is equivalent to obtaining 6 to 10 additional 90 MHz wide frequency allocations in that same band. While these ratios may represent upper bounds, it is clear that a significant increase in spectrum utilization is potentially possible using baseband filtering, even if the ratios are only 3 or 4 to 1. Judging by the auctions now underway in several countries, such additional frequency spectrum will be worth a small fortune and should easily justify expenditures necessary to develop any new filters and/or earth station equipment.

However, baseband filtering is not without problems. Amplitude variations, resulting from data transition density changes found at the output of some of the better performing filters, may make their use difficult with certain modulation types. These variations can be eliminated if Bi-ϕ modulation is used but the required frequency spectrum is increased. Amplitude variations, resulting from the use of baseband filters, may make their use in BPSK/NRZ, QPSK/NRZ, and OQPSK/NRZ systems difficult or impossible, even if these systems have linear modulators. If switched modulators are employed, baseband filtering may not be possible and RF or IF filters will be needed. Further study is required to determine if the amplitude variations can be reduced and to measure their effect on the performance of systems built using each of the modulation methods.

6.0 PHASE 3

Given that baseband filtering has been found to improve the frequency band *Utilization Ratio*, the next step is to apply this technique to each of the modulation schemes identified in Phase 1. New plots, similar to those used in Phase 1, showing *Power Containment* vs. R_B will be generated for comparison with those of Phase 1. At the conclusion of Phase 3, the modulation techniques providing the most efficient frequency spectrum utilization should become clear and the CCSDS and SFCG should be in a position to select preferred methods.

Baseband filter construction will also be considered in greater depth to ensure that the preferred filters can be implemented in a real flight system. Given the apparently superior performance of Raised Cosine filters, further study will be devoted their design, implementation, and performance in a space data system. Compromises in filter design, needed to construct the filters for flight applications, will also be considered.

Earth station detection of the filtered telemetry signal must be investigated to determine the effect of filtering on the telemetry system's performance. While some increase in spacecraft transmitter power might be justified to obtain a significant bandwidth reduction, the extent of such a penalty if it exists, must be computed. Accordingly, end-to-end system performance, including the Inter-Symbol Interference and the Bit-Error-Rate (BER) as a function of E_B/N_0 will be estimated using either actual hardware or by COMDISCO simulation. Strawman designs for the filter, symbol synchronizer, and data detection equipment will be needed.

REFERENCES

1. Martin, W. L. and Tien M. Nguyen, *CCSDS RF and Modulation (Subpanel 1E) Study, A Comparison of Modulation Schemes*, Jet Propulsion Laboratory, Pasadena, California, 24 September 1993.

2. Otter, Manfred, *A Comparison of QPSK, OQPSK, BPSK, and GMSK Modulation Schemes,* European Space Agency, European Space Operations Center, Darmstadt, Germany, June 1994.

3. McGregor, D. N., et. al., *Spectral Characteristics of Digital Phase Modulated Signals,* National Telecommunications Conference, November 1975.

4. Saleh, A. M., *Frequency Independent and Frequency Dependent Nonlinear Models of TWT Amplifiers*, IEEE Transactions on Communications, Vol. COM-29, No.11, November 1981.

5. Saleh, A. M., *Intermodulation Analysis of FDMA Satellite Systems Employing Compensated and Uncompensated TWTs*, IEEE Transactions on Communications, Vol. COM-30, No.5, May 1982.

6. De Gaudenzie, Riccardo *QPSK, OQPSK, MSK, GMSK - A Comparative Performance*
   Evaluation for Space Data Transmission Applications, Consultative Committee for Space Data Systems, Report of the Proceedings of the RF and Modulation Subpanel 1E Meeting at the Ames Research Center, April 11-20, 1989, CCSDS 421.0-G-1, September 1989, p 25.

7. Nguyen, Tien M. and Sami M. Hinedi, *Unbalanced Data Compensation Technique for PCM/PM Receivers,* NASA Tech Brief [to be published].

8. Nguyen, Tien M., *A Review of Current Available Studies for the Interference Susceptibility of Various Modulation Schemes*, "Report of the Proceedings of the RF and Modulation Subpanel 1E Meeting at the GSOC", September 20-24 1993, (Yellow Book) CCSDS B20.0- Y- 1, February 1994.

9. Lucky, R. W., J. Salz, and E. J. Walker Jr., *Principles of Data Communication*, New York: Mc Graw-Hill, 1968, pp 63-65.

10. Proakis, John G., *Digital Communications*, 2nd Edition, New York: Mc Graw-Hill, 1989, pp 528-546.